

WORK PACKAGE: WPLT

DELIVERABLE NUMBER: DEL.4.3

ENVIRONMENTAL IMPACT ASSESSMENT OF D2GRIDS PILOTS

July 2023

Report authors: Stephant Sylvain, Hamm Virginie, Jana Suilen, Eugenia Bueno Martinez

Editing: Eugenia Bueno Martinez

Drawings:

Data sources:

Report done by: BRGM, Open Universiteit

The content reflects the author's views and the Managing Authority is therefore not liable for any use that may be made of the information contained herein.

Table of contents

Table of contents	3
Table of tables.....	4
Table of figures	4
1 Introduction and general approach of the environmental impact assessment	6
1.1 Groundwater impacts.....	6
1.2 CO ₂ emissions and renewable energy	7
1.3 Impacts of heat pumps	7
2 Presentation of pilot sites from D2Grids project	9
2.1 Paris-Saclay pilot presentation	9
2.2 Brunssum pilot presentation	11
2.3 Bochum pilot presentation	12
2.4 Plymouth pilot presentation.....	13
2.5 Glasgow pilot presentation	14
3 Assessment of the process impact on the water quality	16
3.1 Paris-Saclay	16
3.1.1 Description of the natural aquifer.....	16
3.1.1.1 Rock composition.....	16
3.1.1.2 Evolution of the water chemistry	18
3.1.1.3 Characterization of the natural microbial community.....	21
3.1.2 Effect of the temperature variation	22
3.1.2.1 High-pressure experiments.....	22
3.1.2.2 Materials and methods.....	23
3.1.2.3 Results.....	25
3.1.3 Conclusions and recommendations	29
3.2 Brunssum.....	30
3.3 Bochum.....	30
3.3.1 Conclusions and recommendations	31
3.4 Plymouth	32
3.4.1 Conclusions and recommendations	33
3.5 Glasgow	33
4 CO₂ emissions and renewable energy	34
4.1 System boundaries	34
4.2 CO ₂ emissions of pilot sites.....	35

4.2.1	CO ₂ emissions avoidance.....	38
4.3	Share of renewable energy.....	40
4.4	Conclusions and recommendations	42
5	Impacts of heat pumps.....	43
5.1.1	Conclusions and recommendations	45
6	References.....	46

Table of tables

Table 1:	Repartition of the water flow rate according to depth for the GMOU2 well between 657 m and 720 m (Fremont, 2021).	16
Table 2:	Natural water composition measured at several wells of the Paris-Saclay campus.	19
Table 3:	Repartition of the rocks used for the high-pressure experiments and each reactor.	24
Table 4:	Composition of the pumped water from the closed mined “Rober Müser” and “Friedllicher Nachbar” (Seibt, 2021). The water from Rober Müser and Friedllicher Nachbar is respectively pumped at -445 m and -190 m from the surface.....	30
Table 5:	Evolution of the water composition of the PDLBHD(2) well during pumping test (Broadfoot, 2022). ...	33
Table 6 –	Total annual CO _{2eq} emissions and carbon intensity per pilot	36
Table 7.	CO _{2eq} emissions reduced by implementing a 5GDHC system instead of a conventional system.....	39
Table 8.	Overview energy sources used by the different D2Grids pilot projects (non-renewable sources, grey; renewable sources, green). Any backup systems used are not included in this table.....	41
Table 9 –	Performance of the 5GDHC pilot systems regarding different indicators.	42
Table 10 –	Amount of heat pumps with a refrigerant based on HFCs	44
Table 11 –	Total estimated emissions of HFCs in CO _{2eq} emissions and percentage of CO _{2eq} emissions due to leakage of HFCs	44
Table 12 –	Estimated emissions of HFCs in percentage of CO _{2eq} emission reduction	44

Table of figures

Figure 1 -	Design of the DHC network (<i>5GDHC Masterplan & Technical Specifications - Paris-Saclay’s pilot site, 2020</i>).	9
Figure 2:	Map of the Paris-Saclay pilot area. Data are extracted from Geoportail. The considered well for this study are indicated.....	10
Figure 3:	Illustration of the 5GDHC system in Brunssum.	11
Figure 4:	Overview of project Mark 51°7.....	12
Figure 5:	Illustration of the 5GDHC system in Bochum (heating mode – left, cooling mode – right).....	12
Figure 6:	Illustration of the 5GDHC system in Plymouth.	13
Figure 7:	Boreholes location in the pilot area (Broadfoot, 2022).	14
Figure 8.	Illustration of the 5GDHC system in Glasgow	15
Figure 9:	Elemental composition measured by XRF (see section 3.1.2.2.3). Measurements were performed on three rock samples (one color for each one) used for high-pressure experiments. Red lines indicates limits of quantification. “PaF 1025°C” and “PaF 450°C” respectively designate the loss of ignition at 1025°C and 450C.	17

Figure 10: Elemental composition measured by ICP-MS after the rock dissolution (see section 3.1.2.2.3). Measurements were performed on three rock samples (one color for each one) used for the high-pressure experiments. Red lines corresponds to the limit of quantification..... 17

Figure 11: Rock characterization by XRD combined with the Rietveld method. Measurements were performed on three rock samples (one color for each one) used for the high-pressure experiments. 18

Figure 12: Monitoring of the water chemistry of the well n° BSS000RKfZ (Orsay, France). The data were extracted from the ADES database. 20

Figure 13: Relative abundance of main microorganisms detected in GMOU1 water. Three measurements (ESO-1, ESO-2, and ESO3) were performed one after the other. The letters “g-” and “p-” before the microorganisms’ name respectively designate their genus and phylum. 21

Figure 14: Pictures of the BioREP platform. TransREP: simulates reservoirs or fluid transfers. MicroREP: a “lab on chip” device for studying systems at the micrometer scale. CycloREP: designed to characterize leaching processes and solution injectivity through rock. MultiREP: allows both batch and percolation tests simultaneously. 22

Figure 15: Illustration of the BioREP setup used for the high-pressure experiments..... 23

Figure 16: Effect of the temperature on the quantity of feldspar, illite or smectite, kaolinite, and calcite, quantified by XRD. 25

Figure 17: Concentration evolution of Cl, Na, SO₄, and As of the outlet water. 26

Figure 18: Concentration evolution of Ni, Mo, and W of the outlet water. 27

Figure 19: Concentration evolution of Al, Mn, and Ba of the outlet water. 28

Figure 20: High throughput sequencing of high-pressure experiments at 10°C, 30°C, and 50°C. 29

Figure 21. A Hand Dug Well Deriving from the Elizabethan Era – now an ornamental feature in a restaurant... 32

Figure 22. System boundaries of the 5GDHC pilot systems of D2Grids for assessing the environmental impacts of energy use..... 35

Figure 23. CO_{2eq} emissions in of the different 5GDHC pilot systems both with solar PV implemented (dark-shaded) and without (light-shaded) (tCO_{2eq}/yr)..... 37

Figure 24. Carbon intensity of each pilot site (gCO_{2eq}/kWh). With solar PV implemented (dark-shaded) and without (light-shaded) 37

Figure 25. Schematic representation of a reference scenario with heating by individual natural gas boilers and cooling by individual air chillers. 38

Figure 26. Carbon intensity (in gCO_{2eq} fossil/kWh) in the different scenarios for the 5GDHC pilot systems. 39

Figure 27. Share renewable thermal energy sources in the 5G scenario of the pilot systems 41

Figure 28. Share renewable electricity sources (**RERelec**) in the 5G scenario of the pilot systems. 42

1 Introduction and general approach of the environmental impact assessment

This report is divided into three main categories:

1. Groundwater impacts – developed by BRGM in collaboration with pilot sites
2. CO₂ emissions and renewable energy – developed by OU in the form of master's thesis by Jana Suilen
3. Impacts of heat pumps – developed by OU in the form of master's thesis by Jana Suilen

Extracts from the master's thesis are used in this report to represent categories 2 and 3. However, a more extensive in-depth analysis can be found on the thesis itself at research.ou.nl or [e-JES](#).

1.1 Groundwater impacts

This deliverable deals with the methodology used to assess the environmental impact of the subsurface heat storage process developed in some pilots (like Brunssum, Bochum) or studied in Paris Saclay. Each pilot of the D2Grids project is different and uses various underground systems (shallow or deep aquifer, mine water, wastewater) and therefore has its own impacts on the environment, and has to respect policies of its country. That is why it is not possible to apply a common and precise methodology for all pilots as initially defined in LT.4.1. Thus, the aim of this deliverable is to give general principles and guidelines to help each pilot with the environmental impact assessment.

The environmental impact assessment must be applied everywhere the process is taking place. Thus, it concerns:

1. The reservoir where the water is pumped. The main issues are about the diminution of the water level (if the water recharge is not enough), and the modification of the water chemistry and the microbial communities (due to an evolution of the water flow and/or the water level). Hydrogeology and biogeochemistry studies should be performed by considering the other industrial processes in the same area. Data from other wells (water chemistry, pressure, temperature...) and monitored for several years could give precious information about underground systems.
2. The power plant itself. The infrastructures, materials, and quantity of CO₂ avoided... should be considered. It is also important to consider the quality of the pumped water. A high water salinity, the presence of specific bacteria, etc... could enhance the risk of corrosion and clogging.
3. The reservoir where the water is reinjected. It is probably one of the key points as it could highly influence the environment and the process viability. Indeed, the modified water (change in temperature, degassing, bacteria development...) could modify the biogeochemistry of the system.

This report is divided by pilots, for each of these five pilots, the report first focuses on the water quality impacts due to subsurface storage. For Paris-Saclay pilot, complementary experiments and studies were also done and presented here. Moreover, recommendations are proposed for each pilot using ATES systems where data are available. Then, the CO₂ emissions of each pilot are presented. An overview of the project's CO₂ emissions and renewable energy installed is given in a separate section at the end of this report.

1.2 CO₂ emissions and renewable energy

All information regarding CO₂ emissions in this report is gathered from Open Universiteit's master's thesis "Environmental impact assessment of 5th generation district heating and cooling systems" (Suilen, 2023), with permission from the author. Open Universiteit (OU), as partner of the D2Grids project, was in charge of supervising this thesis and gathering all relevant information from pilot sites in order to allow the student to perform the assessment.

Based on the system boundaries defined for each pilot, the energy use in the operational phase of the 5GDHC pilot systems is quantified for each energy source in kWh per year. Subsequently, the impacts of energy use are measured by calculating the share of RES installed and CO_{2eq} emissions for the pilots.

The share of renewable energy implemented in the 5GDHC pilot projects is compared to EU targets regarding renewable energy implementation.

Data needed for assessing the environmental impacts of energy use, have been made available by the different D2Grids pilot projects. However, the pilots are mostly not in full operational state yet, therefore data is mostly based on advanced design plans. For two pilots (Brunssum and Paris-Saclay) operational data is partly available.

Besides the characterization of the systems as they are currently being implemented, an alternative system is used as reference scenario for comparison of the results. In this scenario, the pilot sites are provided energy by conventional heating based on individual gas boilers and cooling by air chillers. Other reference scenarios are also used for comparison, which are not included in this report but can be found in the master's thesis. These include a 4GDHC scenario, a scenario with air-sourced heat-pumps providing all heat and cold, a conventional heating scenario using a CHP for energy generation (both calculated for biomass and natural gas).

The methods of calculating the share of RES, CO_{2eq} emissions and carbon intensity, and the different alternative systems are described in more detail in the master's thesis (Suilen, 2023). There, emissions of local impact pollutants are also calculated.

1.3 Impacts of heat pumps

All information with regards to heat pumps in this report is gathered from Open Universiteit's master's thesis, Suilen (2023), with permission from the author. Open Universiteit (OU), as partner of the D2Grids project, was in charge of supervising this thesis and gathering all relevant information from pilot sites in order to allow the student to perform this assessment.

In this report, we look into the impacts of individual heat pumps, as they play an important role in 5GDHC systems. Heat pumps are electrical devices which convert energy from external heat sources (e.g. air, water and ground) to heat which can be used in residential and commercial buildings for space heating and/or hot water supply (Gaur et al., 2021). For the conversion of heat to the desired temperature (warmer or colder), refrigerants are used. Although heat pumps can lead to reduced carbon emissions and savings in primary energy consumption, this is also dependent of other factors, such as type of technology used, the location and the electricity mix (Gaur et al., 2021, p.1,2). Furthermore, hydrofluorocarbons (HFCs) are often used as refrigerant for in heat pumps (Buffa et al., 2019, p. 507). HFCs are strong GHGs and both Gaur et al. (2021) and Marinelli et al. (2019) name the environmental impacts of these refrigerants, which can be a source of emission and pollution due to potential leakage of the refrigerant. However, Eunomia (2014) find that CO_{2eq} levels of

emissions from leakage are small relative to the total emissions reductions which might be delivered by using heat pump technologies. Their analysis further shows that major impact of refrigerants in heat pumps comes from the ongoing leakage during operation.

The approach that was taken for assessing the impacts of heat pumps in chapter 5 from this report is based mostly on literature review, although there is additional information gathered from the five pilot sites which allowed to perform assumptions for the pilots.

The assessed 5GDHC projects are still under development, and mostly not in full operational state, this means that the data used in this research is often based on assumptions from design plans. If any operational data was already available, it was supplemented with assumptions. Once the pilots are in full operation, which is expected to be between now and 2028, the results could turn out differently. It would therefore be necessary to perform the assessment again, e.g., in five years when more insight in actual performance data is available.

2 Presentation of pilot sites from D2Grids project

2.1 Paris-Saclay pilot presentation

The French pilot is located in the Paris-Saclay campus. It is an urban area where EPA Paris-Saclay is already developing and operating an innovative District Heating and Cooling (DHC) network supplying heat and cold to engineering schools, university buildings, etc... Figure 1 is a schematic view of this network.

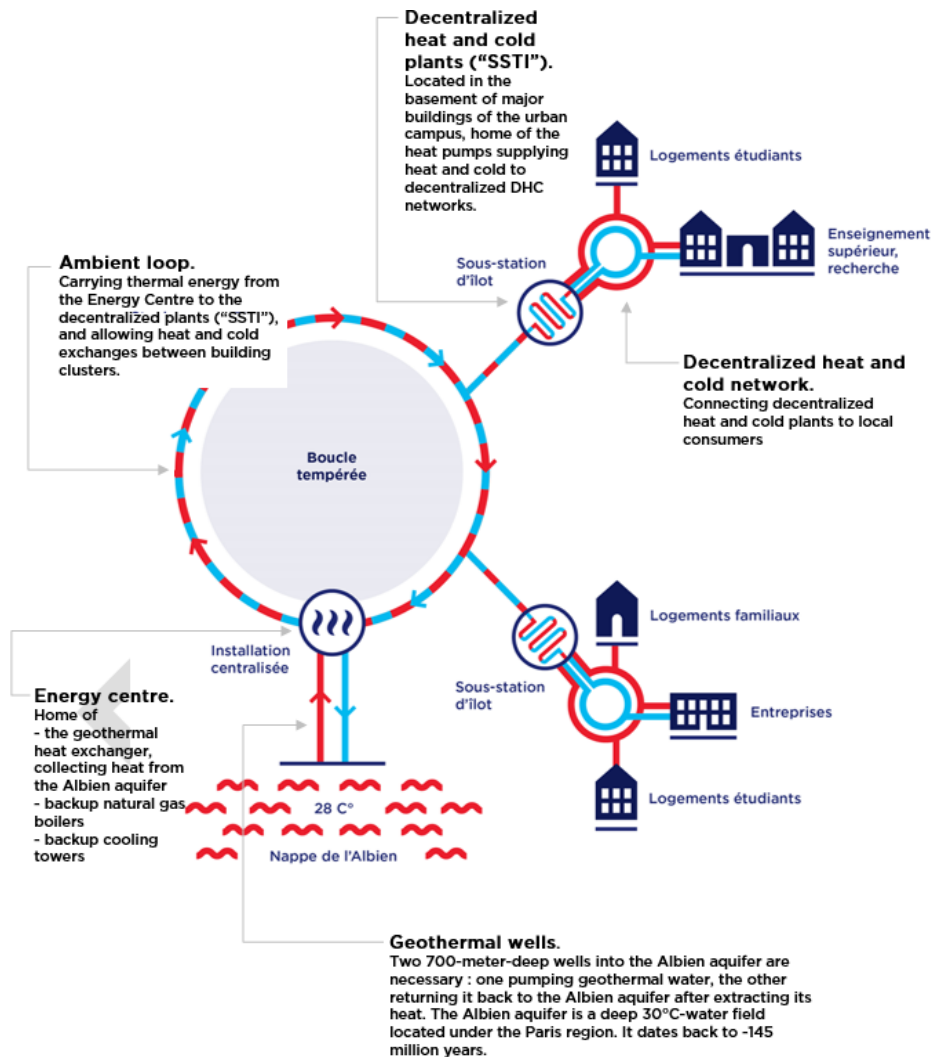


Figure 1 - Design of the DHC network (5GDHC Masterplan & Technical Specifications - Paris-Saclay's pilot site, 2020).

The future DHC network is already composed of two main districts: the Moulon district (“Quartier du Moulon”) and the Ecole Polytechnique district (“Quartier de l’Ecole Polytechnique”), which both accounts for 1 800 000 m² to be built between 2015 and 2030, with the associated infrastructure. Both districts are actually equipped with a geothermal power plant and a doublet (Figure 2):

- GMOU1 (production well) and GMOU2 (injection well) for the Moulon district.
- GEP1 (production well) and GEP2 (injection well) for the Polytechnique district.

Another well is also present in the nearby city of Orsay. This well is used for drinking water purpose.

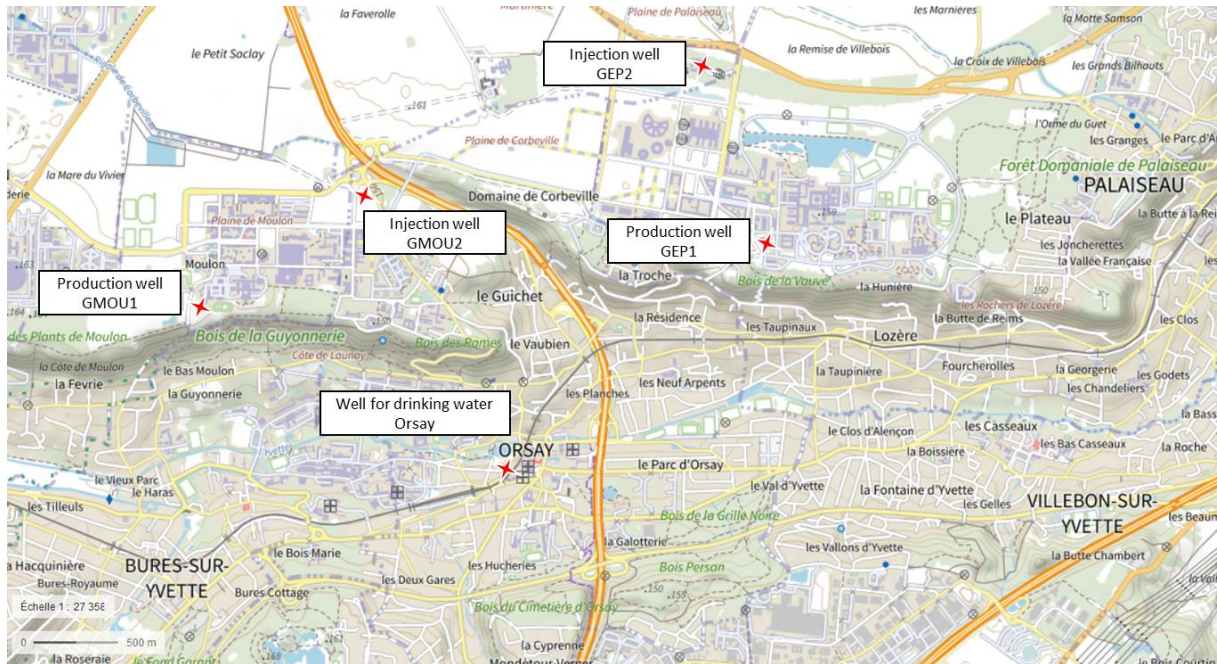


Figure 2: Map of the Paris-Saclay pilot area. Data are extracted from Geoportail. The considered well for this study are indicated.

All these wells are connected to the Albian formation, a sandy multi-layered aquifer, confined in the central part of the Paris Basin. This aquifer covers an area of about 75,000 km² (Vuillaume, 1971) and it is considered strategic for water resources of the Paris area.

In the D2Grids project, the possibility of converting the doublet of the Moulon district for inter-seasonal heat storage in the Albian aquifer is studied. However, this process would generate locally important temperature variations in the aquifer - generating temperatures that can vary from 10°C to 50°C, whereas the natural temperature of the aquifer is naturally at about 30°C. The conventional geothermal doublet already cool down the reservoir temperature around the injection well at 10°C (normal process) but the heat storage process would induce an increase of the reservoir temperature which is not allowed at this time as this water is also used for drinking water purpose (water quality issues). These temperature variations modify the biogeochemical equilibrium (interactions between water, rock and microorganisms) which must be analysed and characterized, to ensure the viability of the process in the long term and the water quality impact in this particular context.

It is within this framework that a series of tests was programmed to characterize the natural environment where the storage could be carried out, and then to study in the laboratory the effects of the temperature variations on the natural environment.

2.2 Brunssum pilot presentation

At the redaction of this report, the Brunssum pilot is a remote mini network which provides heating, cooling, and domestic hot water for around 200 dwellings over 3 apartment blocks (Tarcisius, Oude Egge, and Pastor Savelbergstraat – see Figure 3).

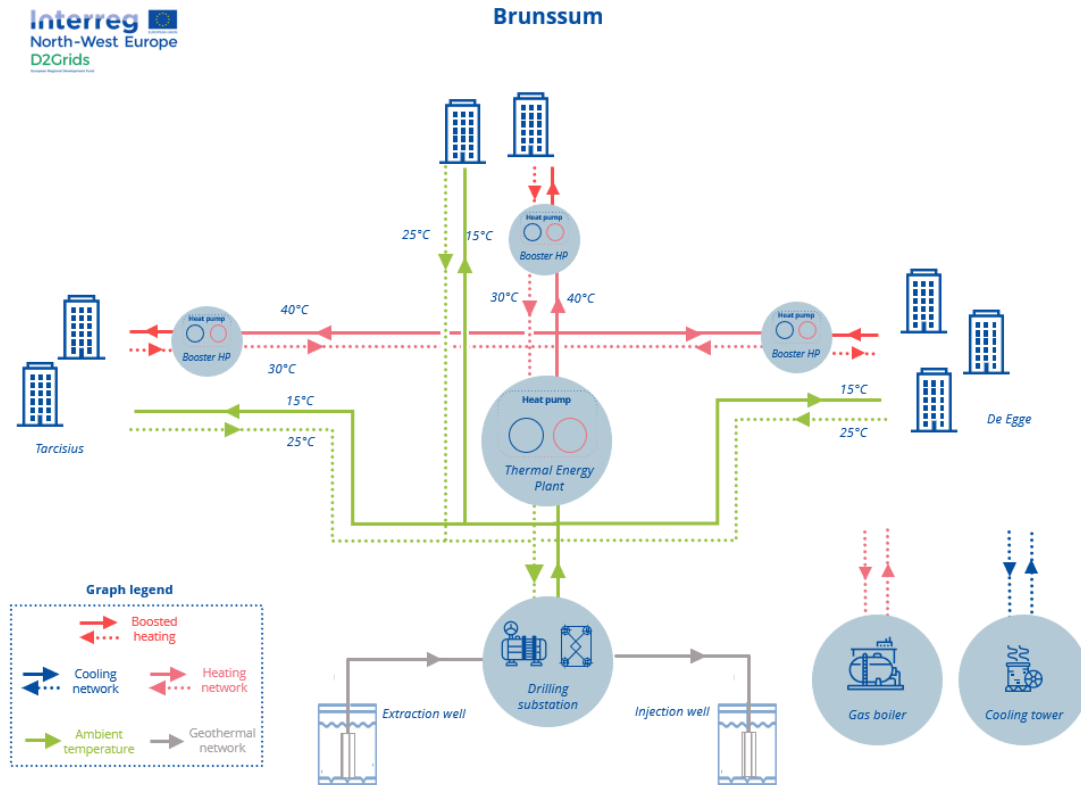


Figure 3: Illustration of the 5GDHC system in Brunssum.

As for the Paris-Saclay Pilot, the Brunssum Pilot use an ATES system combined with heat pumps to provide hot or cool water. The ATES is a two-reservoir system, whereof one is for hot water and one for cold water. The ATES system is at the moment unbalanced, which means that there is more heat extracted from the ATES than is injected back in, which means that it is depleting. To solve this an air-sourced heat pump and dry cooler will be installed to rebalance the ATES.

2.3 Bochum pilot presentation

The 5GDHC system in Bochum will be implemented on the site of the former Opel plant in Bochum, called “Mark 51°7” (Figure 4).

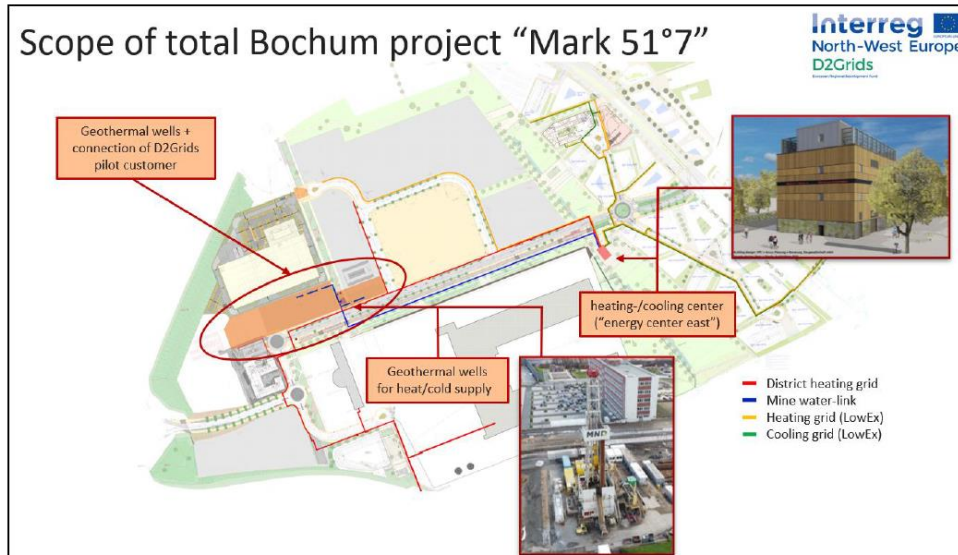


Figure 4: Overview of project Mark 51°7

The district will consist of a broad mixture of new businesses and office buildings, where approximately 25 end-users will be supplied with heat and cold from mine water. The system is expected to run in fully stable state in 2028. Due to former mining activities, there are large mine water reservoirs at a depth of several hundred meters available at the site for thermal storage. One of the wells will be at -820 m of depth from the surface and the other around -340 m. Hydraulic connection will exist between both wells at the surface. The low-grade thermal source of the mine water will fulfil a large part of the heating and cooling demand as environmental source for heat pumps. The system has a connection to a classical district heating network (3G), which would serve to cover peak loads (Figure 5).

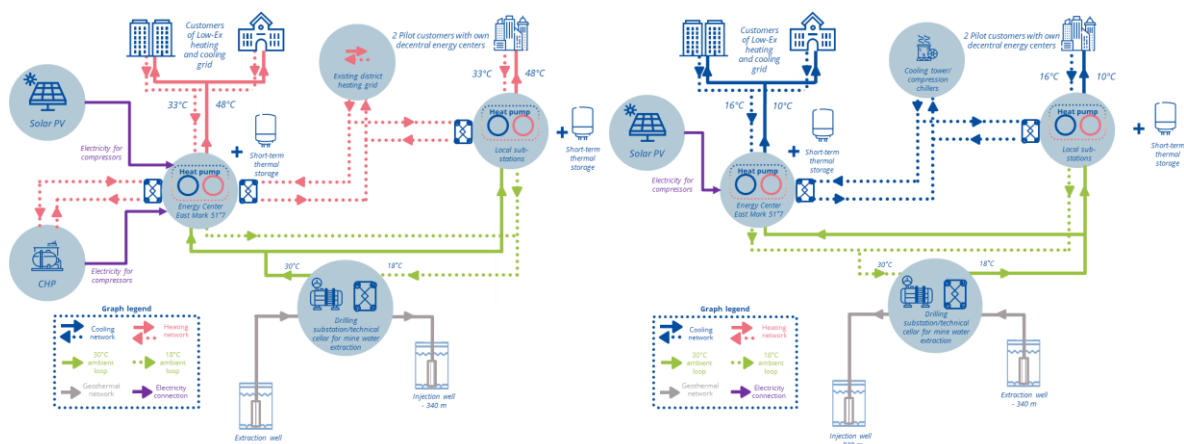


Figure 5: Illustration of the 5GDHC system in Bochum (heating mode – left, cooling mode – right).

2.4 Plymouth pilot presentation

The pilot in Plymouth focuses on two clusters (the Civic and Milbay clusters) in the southern City Centre, which are part of the same masterplan, building on previous work completed under the HeatNet NWE project. It allowed the city to map out heating and cooling loads, identify opportunities for renewable heat sources and develop the concept design of a 5GDHC network (Figure 6).

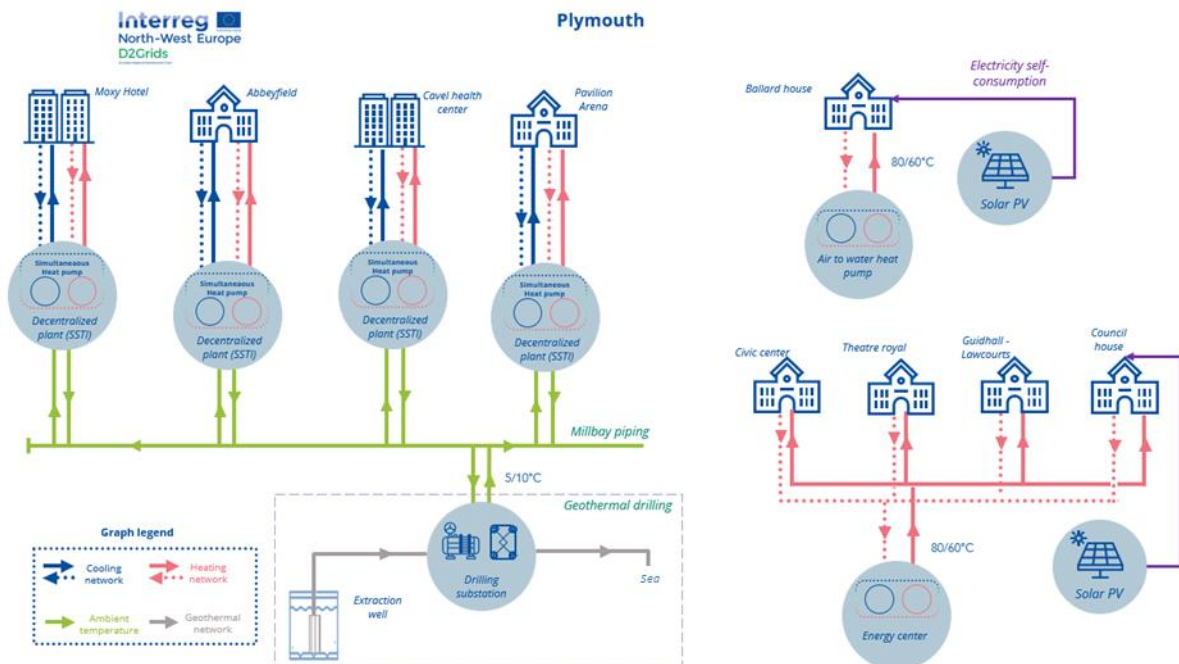


Figure 6: Illustration of the 5GDHC system in Plymouth.

The Civic cluster scheme will deliver a new energy centre (200kW air source heat pump) and one new heat main connection serving three buildings (Guildhall/ Council House and Lawcourts), along with solar PV on the Council House roof connecting to a private wire electricity network. Plans are being developed to expand to connect a mixed-use development at Civic Centre (144 residential units and commercial) and Theatre Royal. These two buildings will also have some cooling loads, with the intention to capture waste heat with storage, where possible.

In the Milbay cluster, the pilot will deliver decentralised heat pumps which are ‘connection ready’ on a new Hotel scheme (currently onsite) but also on an adjacent PCC building (Ballard House) 200kW heat pump together with the solar PV on the roof. The scheme will expand over time to include these buildings but also the adjacent Pavilions events arena, and a new social housing development (147 units) with some commercial. The heat of the district will be obtained with geothermal infrastructure. Groundwater will be pumped from the main aquifer (112 m of depth) and discharged into the sea (Figure 7). Existing wells across this area will be monitored to establish any changes in water level but also salinity and tidal variation, as seawater may also be connected.



Figure 7: Boreholes location in the pilot area (Broadfoot, 2022).

2.5 Glasgow pilot presentation

The Clyde Gateway 5GDHC project is located in the east end of Glasgow and South Lanarkshire. It provides a mix of buildings with a total area of about 11.560 m² with heat and cold. A large part of the thermal energy will be recovered from waste water. When energy from waste water is not available, a gas-fired CHP serves as a back-up.

Clyde Gateway is Scotland’s biggest and most ambitious urban regeneration programme. It is a partnership between Glasgow City Council, South Lanarkshire Council and Scottish Enterprise, backed by funding and direct support from the Scottish Government. It is an important regeneration zone of Glasgow transformed into an area comprising a mix of uses including residential, commercial, retail, leisure and educational buildings.

The project aims to demonstrate its ability to provide an “infrastructure first” solution to energy needs for key masterplan areas which fits as an energy solution over the long term. The objective is to provide low carbon energy but at the same time having technologies which can be attractive to customers and future occupants of the buildings.

The provision of an electric grid connection will seek to supply up to 2MW of power over the short term of the project to support integration with the thermal grid. A key goal is to demonstrate the viability of the initial project and its capability of scaling up with modular growth. The intention is to show this technically as an efficient system solution and through the commercial financial model in terms of sustainability.

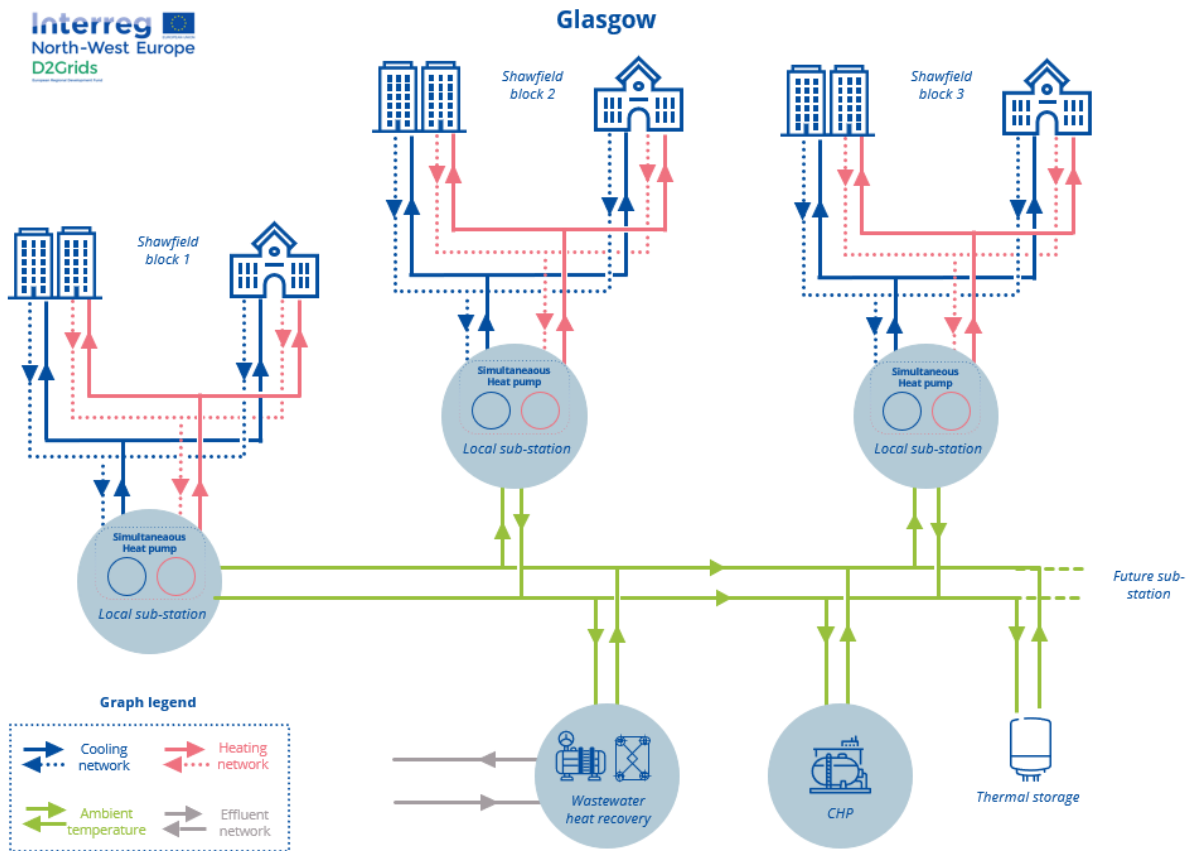


Figure 8. Illustration of the 5GDHC system in Glasgow

The site is made of three buildings:

- The Red Tree Magenta, which is already existing, and is a multi-tenanted office building
- The Red Tree Central, which is to be built, and is a new 4-storey office building
- The Red Tree Technology Hub, also to be built, is a new 2-storey building containing a mixture of office and workshop spaces.

The 5GDHC grid will provide low-graded energy to the 3 buildings located in the Shawfield Development area which has been earmarked for mainly commercial use. The Shawfield Development zone is a pre-industrial site located in the west of the River Clyde. Using this process, the first building which will benefit from this 5GDHC grid will be "Red Tree Magenta" in July 2023. In the long run, the entire business park should be connected to the grid.

3 Assessment of the process impact on the water quality

3.1 Paris-Saclay

3.1.1 Description of the natural aquifer

3.1.1.1 Rock composition

The Albian formation is mainly composed of quartz sand, associated with glauconite, kaolinite, muscovite, carbonates (siderite, calcite, and dolomite), phosphates, barite and pyrite (Mégnyen and Mégnyen, 1980). The rock properties (minerals proportion, microstructure, permeability...) evolve according to the depth and the area. For example, Table 1 shows the flow rate variation according to the depth. The maximum measured flow rate was obtained between 657 m and 720 m of depth for the GMOU2 well (Table 1). For this reason, we focused the mineralogical characterisation on the most productive layers. Several rock samples from these depths were taken and mixed before to be analysed (see section 3.1.2.2.1 for more details).

Table 1: Repartition of the water flow rate according to depth for the GMOU2 well between 657 m and 720 m (Fremont, 2021).

Considered level (depth to the surface – m)	Thickness (m)	%of the total flow rate
657.5 - 658.7	1	0.6
665.3 - 668.1	2.9	5.6
669.2 - 671.5	2.2	19.2
681.2 - 683.0	1.9	6.1
685.5 - 685.8	0.3	4.3
687.2 - 689.4	2.2	4.1
715.2 - 722.0	6.8	60.1

The sampled rocks were composed of 95 (%wt) of silicate, calcium, iron, and magnesium oxides (see Figure 9 and Figure 10). XRD results (see Figure 11) indicated that these elements were mainly contained in quartz (SiO₂), and potassium feldspar (KAlSi₃O₈: microcline or orthoclase). A small amount of illite or smectite, kaolinite, apatite, micas, and calcite were also detected by XRD. SEM observation also revealed the presence of barite, pyrite and iron oxide. Inclusion of zirconium and titanium were also detected.

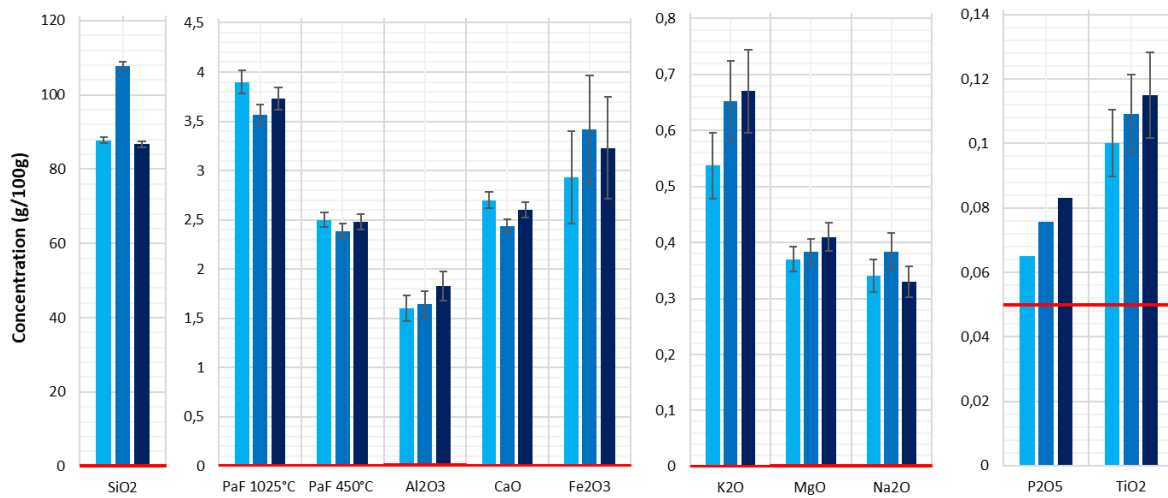


Figure 9: Elemental composition measured by XRF (see section 3.1.2.2.3). Measurements were performed on three rock samples (one color for each one) used for high-pressure experiments. Red lines indicates limits of quantification. “PaF 1025°C” and “PaF 450°C” respectively designate the loss of ignition at 1025°C and 450C.

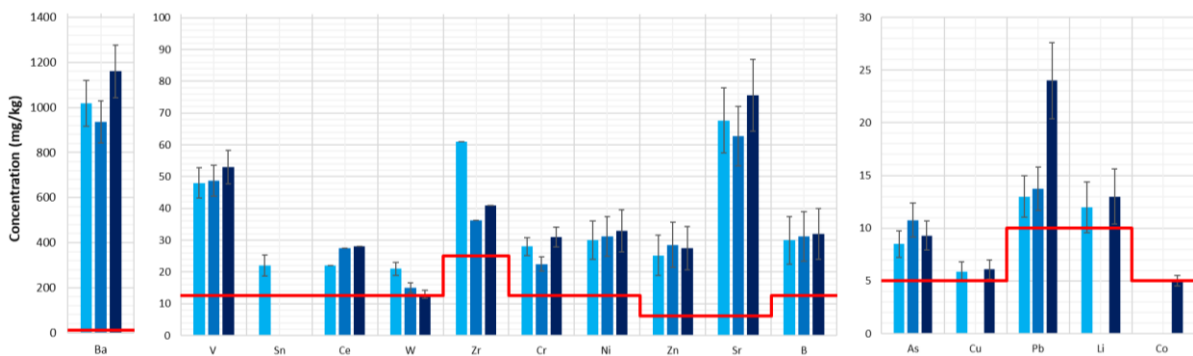


Figure 10: Elemental composition measured by ICP-MS after the rock dissolution (see section 3.1.2.2.3). Measurements were performed on three rock samples (one color for each one) used for the high-pressure experiments. Red lines corresponds to the limit of quantification.

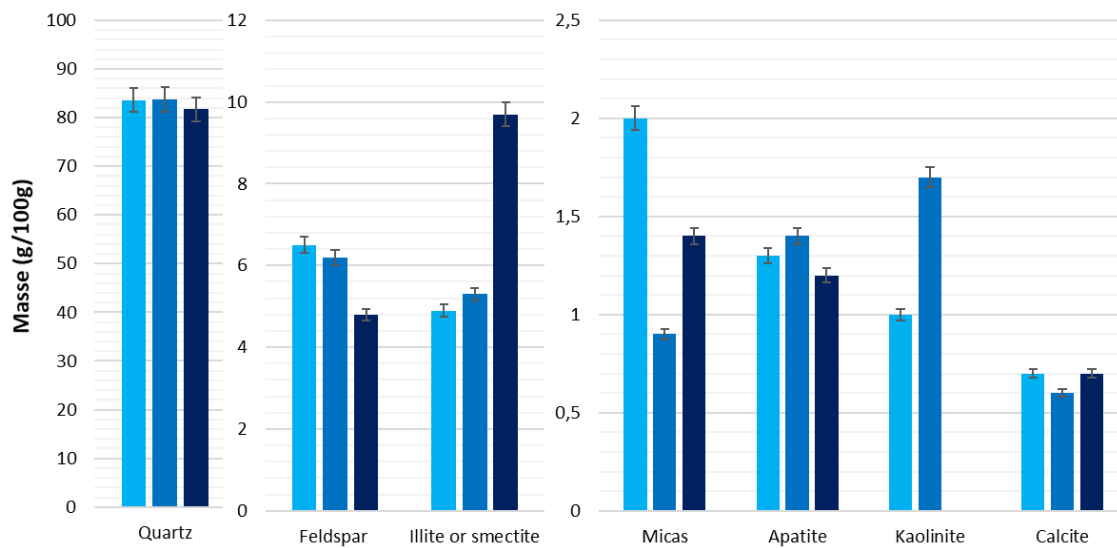


Figure 11: Rock characterization by XRD combined with the Rietveld method. Measurements were performed on three rock samples (one color for each one) used for the high-pressure experiments.

3.1.1.2 Evolution of the water chemistry

The Albian aquifer is a confined aquifer characterized by high water reserves, and a very low natural recharge compared to its total volume. The chemical composition of the fresh groundwater in the Albian formation varies throughout the aquifer, resulting from a complex hydrogeology with multiple recharge components and residence times (Raoult et al., 1997).

Water analyses were performed at several places and times to characterize the aquifer geochemistry and the water composition variability in the area (Figure 2).

The natural water has a low salinity (around 253 mg/L) with a $\text{Ca-SO}_4\text{-HCO}_3$ facies. The pH is around 7.4 and the redox potential is -248 mV (Ag/AgCl), which is coherent with the low oxygen content. The calculation of the saturation indices with the Phreeqc software and the Thermoddem database (Blanc et al., 2012) indicated the water is close to the equilibrium of the main phases identified by XRD (i.e. quartz, feldspar, smectite, illite, kaolinite, and calcite) and SEM (barite). The sulfur speciation was not characterized but the negative redox potential and the presence of pyrite suggest the presence of sulfide. Iron was initially present as Fe(III). Water chemistry of GMOU1 and Orsay are closed. Analyses of the well GEP1 are occurring and will allow concluding about spatial variability.

Table 2: Natural water composition measured at several wells of the Paris-Saclay campus.

Chemical species	GMOU1	Orsay	Unit
Date	04/2021	04/2022 (ADES database)	
Ca	34.1	31	mg/L
K	8.9	9	
Fe	0.21	0.22	
Mg	8.1	6.3	
Na	7.8	5.5	
Si	13.5	13	
HCO ₃	148	131	
F	0.43	0.16	
Cl	8.1	4.8	
SO ₄	17.5	11	
NH ₄	0.05	0.14	
Al	1.62	3.7	
B	56.3	19.4	
Ba	39.1	26.9	
Cu	0.15		
Li	9.57		
Mn	55	28.8	
Ni	0.3		
Sr	655		
Zn	1.83		
As	1.07	1.38	
Ti	0.1	0.11	
Mo	0.231		
Rb	7.35		
W	0.056		
pH	7.4	7.8	
Conductivity	260	255	µS/cm
Oxygen saturation	1		%
Eh	-248		mV – Ag/AgCl

As explained previously, the Albian aquifer is used for drinking water. Orsay city pumped this water for several years and has to monitor its quality (Figure 12). As the pumped well is very close to the Paris-Saclay pilot (around 3 km), this well gives an opportunity to study the water chemistry evolution according to the time.

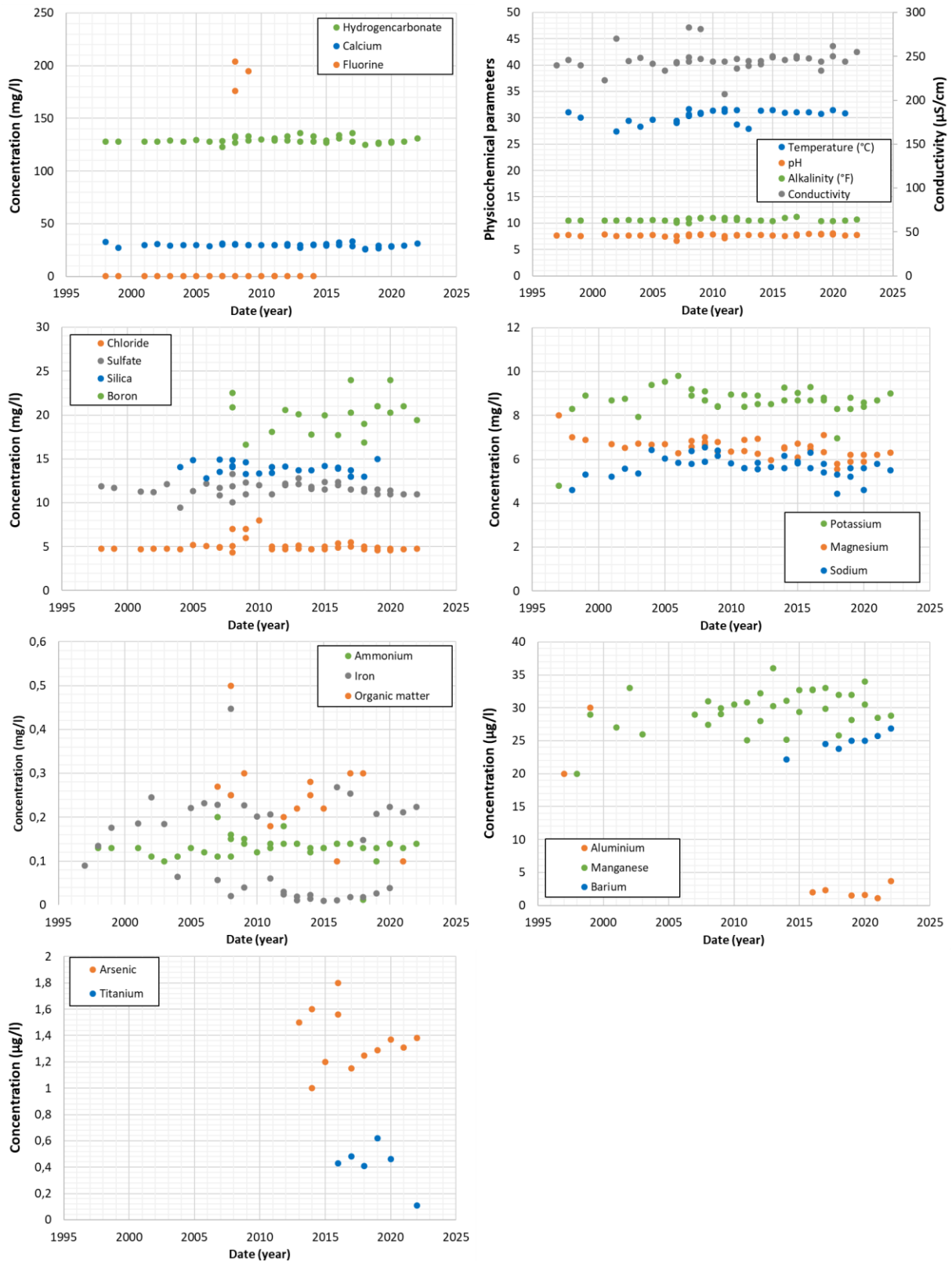


Figure 12: Monitoring of the water chemistry of the well n° BSS00RKZ (Orsay, France). The data were extracted from the ADES database.

Most of the physicochemical parameters that have been measured during the last twenty years underlined a low evolution of the water composition. The values dispersion of the major and minor element concentrations were very low, and are in agreement with the measured values (Table 2). A slight discrepancy can be observed around 2008 for fluorine, conductivity and iron. As these variations only occurred for one or two years, we supposed these changes were due to maintenance procedures or inappropriate water analysis. Variations are more important for trace elements and some differences (mainly for boron, manganese and barium) can be underlined, probably because of a different sampling/measurement procedure. For example, Iron can be oxidized by oxygen and precipitate after the water sampling. No variation of the water composition was observed after the pumping

3.1.1.3 Characterization of the natural microbial community

The microbial diversity of the Albian aquifer was poorly studied. This is why, water was filtrated to collect microorganisms and perform high throughput sequencing (see 3.1.2.2.4). A first analysis was performed in 2021 at the same time than water sampling (Figure 13).

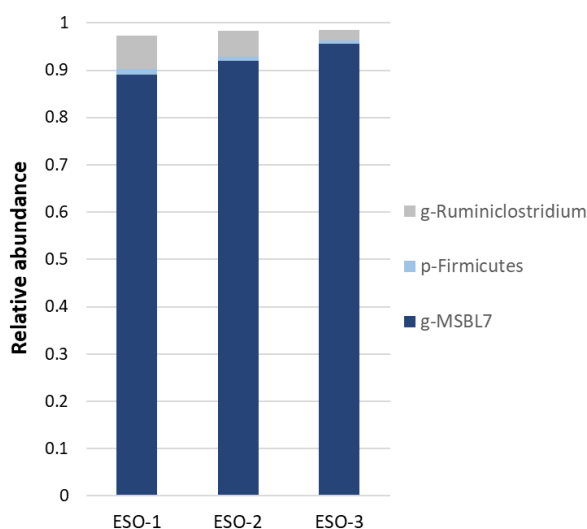


Figure 13: Relative abundance of main microorganisms detected in GMOU1 water. Three measurements (ESO-1, ESO-2, and ESO3) were performed one after the other. The letters “g-” and “p-” before the microorganisms’ name respectively designate their genus and phylum.

The results highlights the predominance of 3 taxon that represent 97% of the diversity that are often ascribed to the degradation of organic matter and the reduction of sulfate (Galushko and Kuever, 2020; Häusler et al., 2014; Wu and Cheng, 2021). The low microbial diversity of the sample suggests the results are possibly not representative of natural microbial diversity in the aquifer. This diversity could be due to corrosion processes (in the pipe for example) as sulfate reduction bacteria are often linked to these processes. This assumption is supported by the fact maintenance procedure were occurring some weeks before water sampling and another study highlight a higher diversity (Ungemach and Souque, 2021). Other analyses are occurring at the redaction of this deliverable.

3.1.2 Effect of the temperature variation

As indicated previously, the aquifer thermal energy storage process will modify the temperature of the aquifer. The process could generating temperatures that can vary from 10°C to 50°C, whereas the natural temperature of the aquifer is naturally at about 30°C. These temperature variations would then modify the biogeochemical equilibrium (interactions between water, rock and microorganisms) which must be analysed and characterised, to ensure the viability of the process and the impact on the water quality. For this purpose, high-pressure experiments were performed with the BioREP plateform to mimic the aquifer thermal energy storage process.

3.1.2.1 High-pressure experiments

The BioREP platform were used to perform the high-pressure experiments. This experimental platform was developed for studying and characterising the natural biogeochemical and/or industrial processes that take place in deep geological environments. It enables the safe study of interactions between water, gas, rocks and microorganisms under a wide range of pressures and temperatures, for both fundamental research and very specific operational needs.

The platform consists of several reactors, transfer columns and other tools (pumps, sensors, etc.) that can be modulated and combined *ad infinitum* to perform customized tests (Figure 14). Each reactor is equipped with several sensors allowing precise monitoring of the environment (pH, Eh, pressure, temperature, gas consumption, flow rate, etc.). Particular attention was paid to the choice of materials in order to ensure the inertia of the system from a chemical and microbiological point of view. Specific sampling procedures were also implemented to enable working in anoxic conditions, and to take samples in safety conditions, while limiting the risk of pollution of the environment and lethality of microorganisms due to decompression.

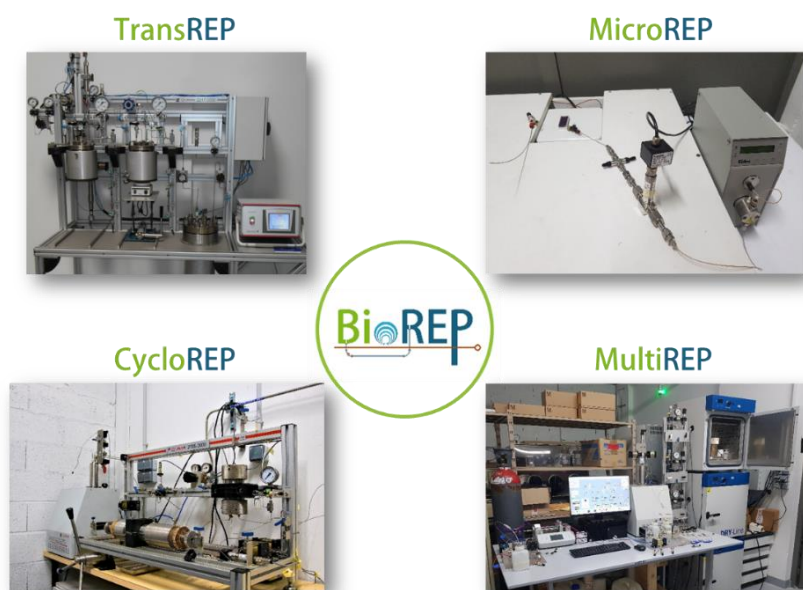


Figure 14: Pictures of the BioREP platform. TransREP: simulates reservoirs or fluid transfers. MicroREP: a “lab on chip” device for studying systems at the micrometer scale. CycloREP: designed to characterize leaching

processes and solution injectivity through rock. MultiREP: allows both batch and percolation tests simultaneously.

The MultiREP set up was used in the present study as it allows performing several percolation experiments simultaneously (Figure 15).

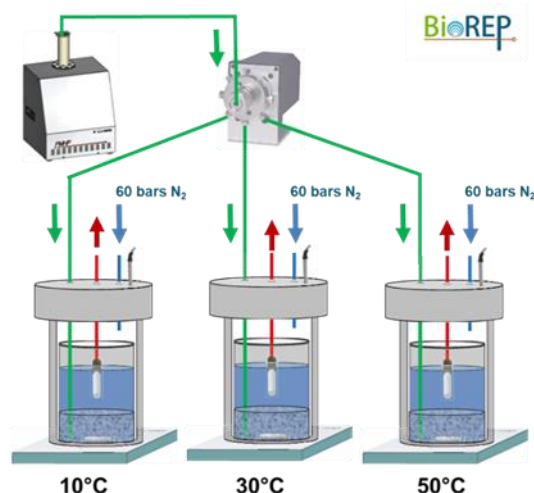


Figure 15: Illustration of the BioREP setup used for the high-pressure experiments.

Before any tests, the major parts (pipes) of the device were sterilized at 120°C for 20 min. The other parts (valves and a high-pressure pump) were washed with nitric acid (10%) and ethanol (70%) for 24h. Sterilized water was finally used to rinse the setup. In parallel of these steps, each reactor was filled with 75 g of natural rocks (see the section 3.1.2.2.1 for more details). Then, reactors (and thus the natural rock) were also sterilized every 24 hours at 120°C for 20 min, during three days.

Natural water containers (see the section 3.1.2.2.1 for more details) were connected to the BioREP set up with a sterilized tube and maintained at 1.5 bar (absolute pressure) of nitrogen to avoid depressurization and oxygen contamination. Natural water was injected with a flow rate of 1 mL/min into three reactors in parallel filled with rock.

At the beginning of the experiment, the three reactors were kept at 30°C for one week. Then, the temperature was increased to 50°C in the first reactor and decreased to 10°C in the second one. The last one was kept at 30°C as a reference. Geochemical processes were monitored by: (1) analysing the outlet water (see section 3.1.2.2.2) throughout the experiments, (2) characterizing the rock composition (see section 3.1.2.2.3) before and after the experiments, and (3) identifying the taxonomic diversity of microbial communities (see section 3.1.2.2.4) at the end of the experiments. Experiments were stopped after 28 days.

3.1.2.2 Materials and methods

3.1.2.2.1 Water and rock sampling

Rocks used for the high-pressure experiments were sampled during the drilling of the producing well of the geothermal power plant of Paris Saclay. Rocks were sampled between 655 m and 726 m of depth (to the surface).

This level corresponds to the well strainer and the lower Albian geological formation. The rock is non-consolidated and is mainly composed of sands and clays (see section 3.1.1.1). The different rock samples were mixed for the high-pressure experiments to be the most representative as possible of the aquifer (Table 3).

Table 3: Repartition of the rocks used for the high-pressure experiments and each reactor.

Depth (m)	Reactor at 50°C	Reactor at 30°C	Reactor at 10°C
665	10.45	10.50	10.51
675	20.95	20.90	20.98
680	12.01	12.02	12.04
685	6.35	6.32	6.33
695	4.83	4.80	4.81
705	9.70	9.75	9.64
725	10.03	10.10	9.96

Natural water was used for the flow-through experiments. It was sampled at the geothermal power plant at the top of the producing well (GMOU1 – see Table 2). Water was stored in sterilized and airtight (with rubber stopper) containers of 20 L. Containers were then filled with nitrogen to limit water oxidation.

3.1.2.2.2 Water analyses

The solutions collected at the output were filtered (<0.2 µm). Cl, F, NO₃ and SO₄ concentrations were measured using ion chromatography (Thermo-Dionex ICS3000; detection limits = 0.5 mg/L). Ca, Fe, K, Mg, Na, S_{tot} and Si were measured by ICP-AES (OPTIMA 5300 DV, Perkin Elmer; dl = 0.5 mg/L for all elements). Trace elements (Al, B, Ba, Cu, Li, Mn, Ni, Sr, Zn, As, Ti, Mo, Br, Rb, W, and Zr) were determined by ICP-MS (NEXION 350 X, Perkin Elmer; dl = 0.5 µg/L and 0.1 µg/L for Al and Cu, respectively). Moreover, HCO₃ and CO₃ were analysed by potentiometry, and NH₄, NO₂ and PO₄ were analysed by UV-Visible.

3.1.2.2.3 Solid analyses

The rock elemental compositions was determined by combining X-ray fluorescence analyses for major elements and ICP-AES measurements after the rock dissolution in sodium peroxide and chloride acid solution (33%) for trace elements. The analyzed elements were Ag, Al₂O₃, As, B, Ba, Be, Bi, CaO, Cd, Ce, Co, Cr, Cu, Fe₂O₃, K₂O, La, Li, MgO, MnO, Mo, Nb, Ni, P₂O₅, Pb, Sb, SiO₂, Sn, Sr, TiO₂, V, W, Y, Zn, and Zr. Results were normalized to the initial rock.

Crystalline phases were also characterized and quantified by X-ray diffraction. Analyses were performed on powdered rock with a Bruker D8 Advance diffractometer in a θ - θ configuration employing Cu K α radiation ($\lambda=1.541$ Å) with a rotating sample stage. The samples were scanned between 4 and 75°. Each step size was acquired for 556.8 seconds at a scan speed of 0.03°2 θ /second. X-ray diffraction patterns were qualitatively analyzed with the Diffrac SuiteTM software. Rietveld refinement was then performed on the X-ray powder pattern by using the SiroQuant V.4 program from Sietronics.

The mineralogical characterization was completed by Scanning Electron Microscopy (SEM) observations coupled with a Secondary Electrons (SE) detector, a BackScattered Electrons (BSE) detector, and a Energy Dispersive X-Ray (EDS) detector. The goal of these analyses was to identify other minerals present in too low concentration in the rock to be detected by XRD.

3.1.2.2.4 Microbial analyses

Biomolecular analyses were performed on DNA from water and rock samples at the end of the high-pressure experiments. Five hundred mL of the outlet solution were filtered at 0.2 μm in sterile conditions for each reactor to recover microbial biomass, and filters were stored at -20 °C before DNA extraction. Moreover, 5 g of rock sampled from along the core were stored at - 20°C and subsampled into 1 g aliquots for DNA extraction. Microbial DNA was extracted from frozen filters (cut with a sterile scalpel) and rock samples with the FastDNA™ SPIN Kit for Soil and the FastPrep®-24 instrument. according to the manufacturer’s instructions (MP Biomedicals) and applying a speed of 5 m/s balance. Metabarcoding on the 16S rRNA genes V4-V5 region was performed using universal primers 515WF/928WR and Illumina MiSeq sequencing, and the FROGS bioinformatics pipeline (Escudié et al., 2018) for pair-end reads quality filtering, OTU curation, and taxonomic assignment.

3.1.2.3 Results

3.1.2.3.1 Geochemistry

The main effect of the process was the rock lixiviation due to the water flow. The temperature variation itself (i.e. 10°C, 30°C, and 50°C) had a relatively low impact on the geochemistry. A small increase in the calcite and illite/smectite could be observed with the temperature augmentation (see Figure 16). On the opposite, the kaolinite and the feldspar content decreased with a lower temperature. Except for the illite/smectite, these results are in agreement with saturation indices evolution.

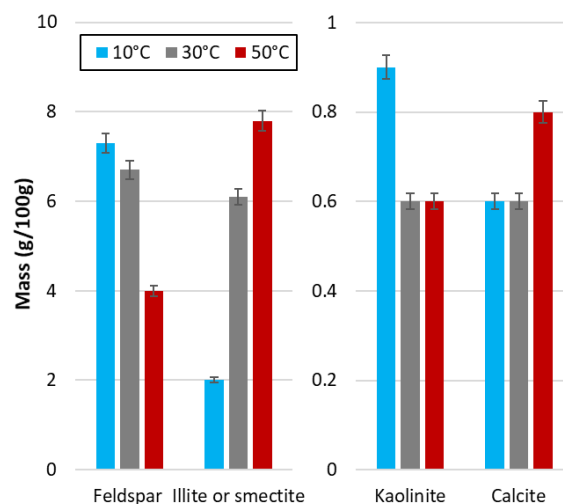


Figure 16: Effect of the temperature on the quantity of feldspar, illite or smectite, kaolinite, and calcite, quantified by XRD.

These mineralogical changes are difficult to correlate with the water composition because the water flow diluted elements. Indeed, most of the major and trace elements were not significantly impacted during the tests. However, the concentration of several ionic species evolved and can be classified into three groups. The first group concerns Cl, Na, SO_4^{2-} and As. High concentrations of these elements were detected at the beginning of the percolation before dropping (Figure 17). This quick dissolution was probably due to the presence of residual salts such as NaCl coming from fluids used for the well drilling.

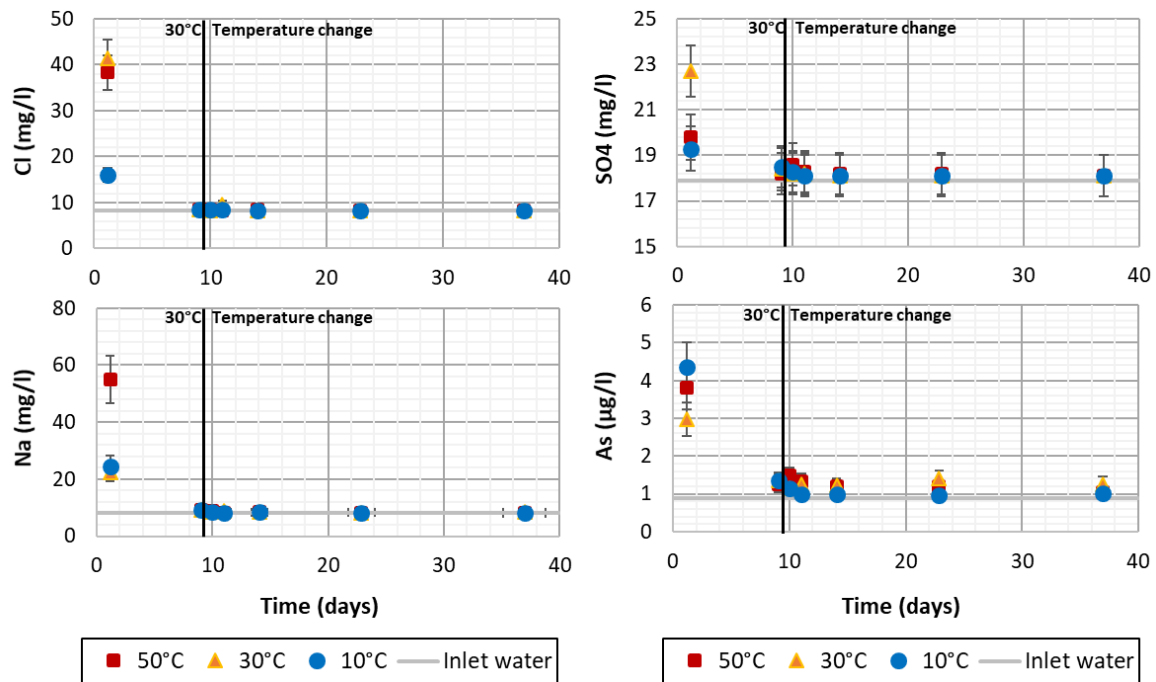


Figure 17: Concentration evolution of Cl, Na, SO_4 , and As of the outlet water.

In the second group, a progressive augmentation of the concentrations of Ni, Mo, and W was observed after the temperature equilibration (Figure 18). Then, their concentrations decreased for the last measurement point. These variations could be due to the desorption from clay or a progressive and complete dissolution of minerals. However, SEM observation did not allow identifying these phases yet.

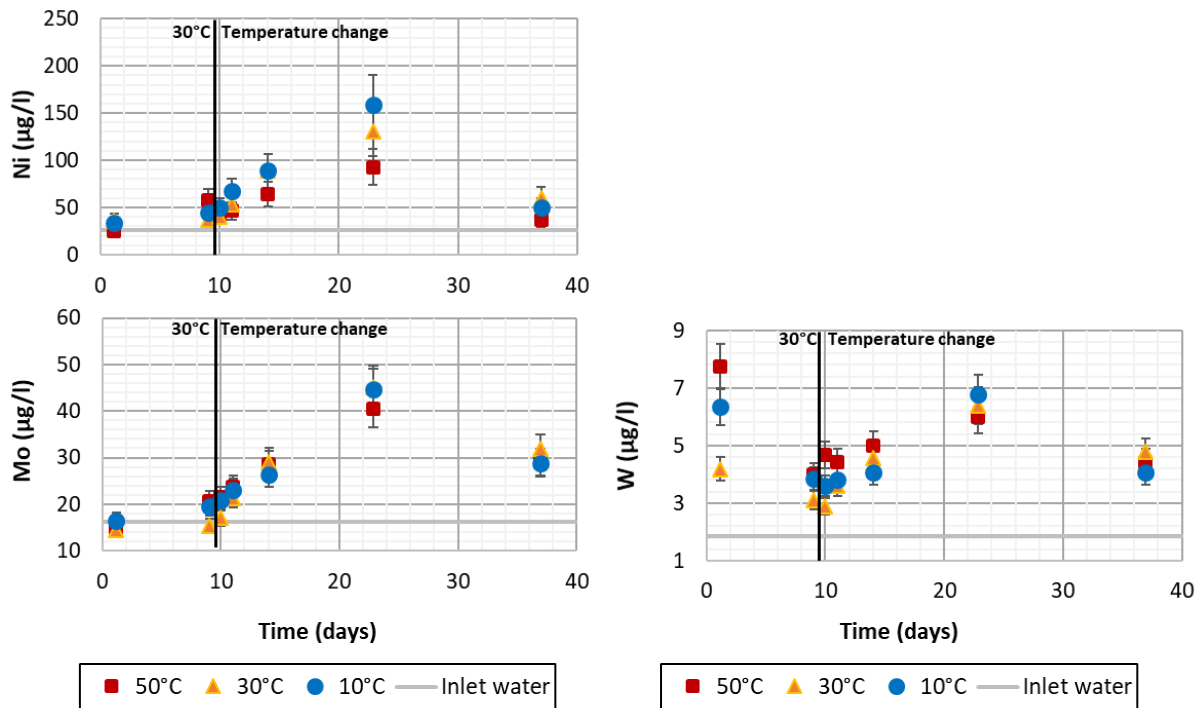


Figure 18: Concentration evolution of Ni, Mo, and W of the outlet water.

In the last group, the concentration of the species varied according to the time and the temperature. Aluminum concentration decreased at 10°C and 30°C whereas it stayed constant at 50°C. The manganese concentration was systemically higher at 10°C. On the opposite, the barium concentration increased with the temperature. These evolutions are in agreement with thermodynamic simulations if we suppose the presence of barite (for the barium), ferrite or jacobite (for manganese), and feldspar, smectite or illite (for aluminum). Further analyses are necessary to better identify the phases relied on these elements.

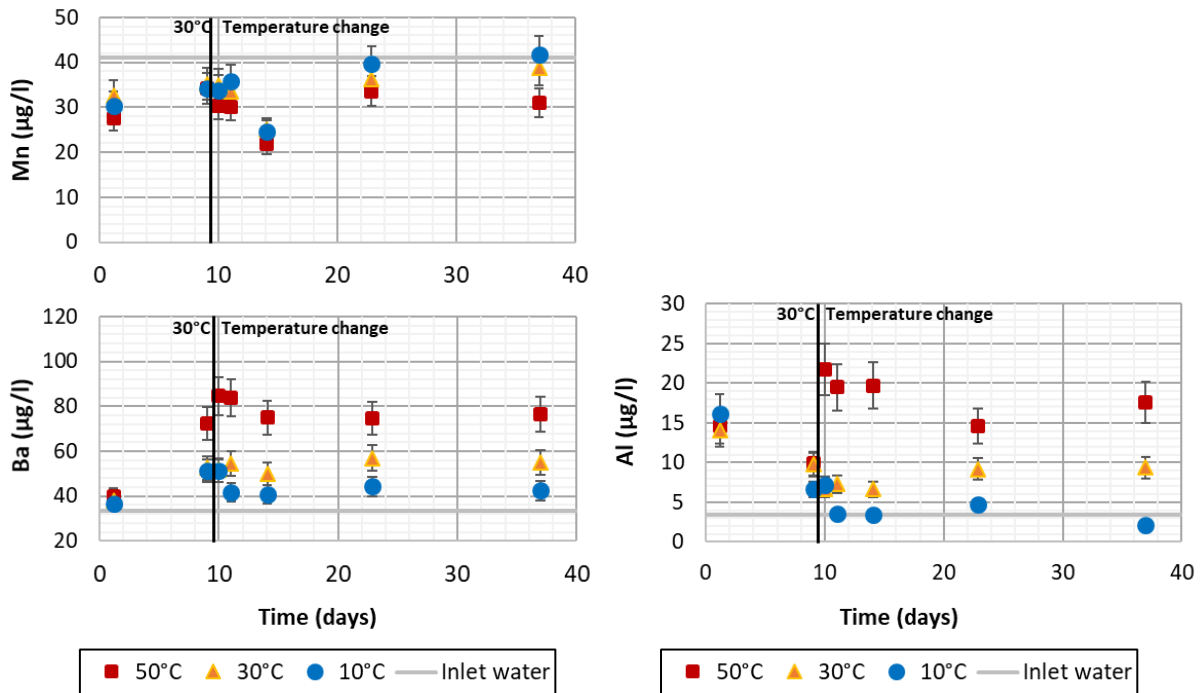


Figure 19: Concentration evolution of Al, Mn, and Ba of the outlet water.

3.1.2.3.2 Microbiology

The temperature difference between reactors induced a high variation of the bacteria diversity. The same main genus can be identified for all the temperature but relative sequence abundance are different.

At 30°C (the natural temperature of the aquifer) there was not a clear dominance of a genus. The genera *Methyloversatilis*, *Lacunisphaera*, *Obscuribacter*, and *Aquabacterium* were all present between 5% to 15%, as well as members of the families *Rhodocyclaceae* and *Opotutaceae*.

The diminution of the temperature at 10°C favoured the genus *Aquabacterium* and members of the *Pseudomonadales* order and the *Comamonadaceae* family. Indeed, these taxa represent until 80% of the detected sequences.

On the opposite, the temperature augmentation (50°C) favoured the *Methyloversatilis* genus as it represents 70% of the sequences.

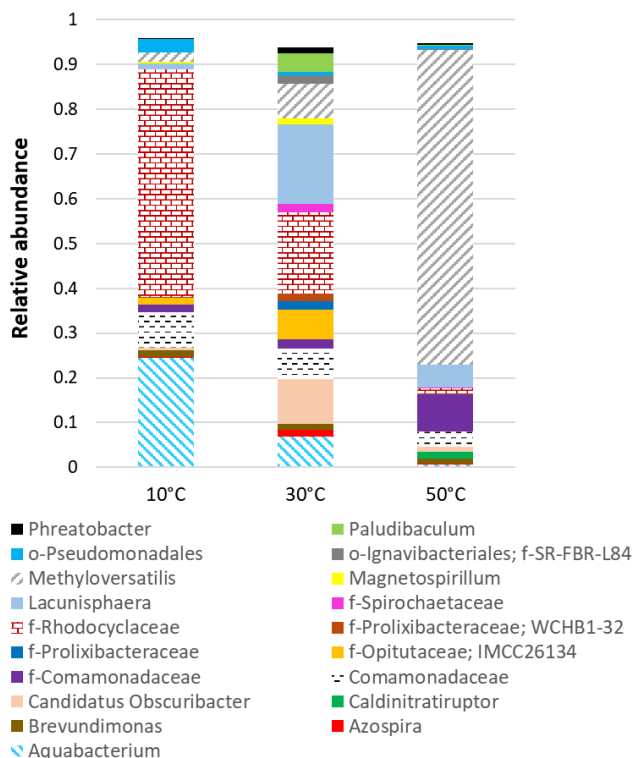


Figure 20: High throughput sequencing of high-pressure experiments at 10°C, 30°C, and 50°C.

All the identified genera are usually attributed to bacteria coming from groundwater, freshwater, or sediments (Fardeau *et al.*, 2010 ; Garrity *et al.*, 2015 ; Iino, 2018 ; Kalyuzhnaya *et al.*, 2006 ; Manz *et al.*, 2015 ; Rast *et al.*, 2017 ; Schöler et Schleifer, 2015 ; Vancanneyt *et al.*, 2005 ; Willems et Gillis, 2015). The optimum living conditions for these microorganisms are comprised between 5°C to 60°C for the temperature, 5.5 to 8 for the pH, and a relatively low salinity. These results are thus in agreement with conditions prevailing in our experiments.

A wide range of functions are known to be carried by some of the detected bacteria. A major part of them is able to reduce oxygen, nitrate, and iron, and to use inorganic or organic carbon to grow. This task is still occurring at the redaction of this work.

3.1.3 Conclusions and recommendations

A first evaluation of the environmental impact of the Aquifer Thermal Energy Storage (ATES) was performed by (1) characterizing the natural environment, and (2) performing high-pressure experiments to mimic the ATES process.

The Albian aquifer is already used for geothermal processes and for drinking water. These existing infrastructures allow having geochemical data for several years. Geothermal plants seem to have a low impact on the main chemical species. Higher variations were observed for trace elements.

There were very little data about the microorganisms present in the aquifer. This is why, analyses were performed at several places and at different times. At the redaction of this document, analyses are still occurring. The characterization of the natural microbial diversity should be complemented with these analyses and with further campaigns.

Laboratory tests did not highlight a strong impact of temperature variation on geochemistry. The impact of the microbial diversity was much higher. It is important to note these tests only occurred for 28 days at a laboratory scale and could not be representative of the reservoir and long-term processes. Longer experiments or modelling of the process (at the laboratory and upper scale) would complete the assessment of the geochemical evolution. Moreover, the high-pressure experiments did not reproduce the cycling of the process (inversion of the flow rate according to the seasons). The process reversibility could enhance biogeochemical processes that have to be assessed.

A first evaluation of the microbial functions has been done in the project according to the existing data in the literature. These microorganisms are classically observed in aquifer systems and for this range of temperatures. It is now necessary to determine if these microorganisms can have a role in corrosion and clogging issues. Moreover, no evidence of pathogenic bacteria was highlighted during these tests whatever the water temperature. However, the performed experiments were not dedicated to highlight these kind of microorganisms. Complementary analyses are this necessary to study this point.

3.2 Brunssum

At the redaction of this deliverable and at the authors' knowledge the water chemistry is partially known and the microbial diversity have not been characterized yet. It is necessary to acquire a biogeochemical baseline of the aquifer before asses the process impact. The goal of this step is to characterize the spatial and temporal variation that occur in the natural environment.

3.3 Bochum

At the redaction of this document, the water chemistry of each well is not known. However, waters from closed mines in the same area (see Figure 4) are continuously pumped and analysed (Table 4).

Table 4: Composition of the pumped water from the closed mined “Rober Müser” and “Friedllicher Nachbar” (Seibt, 2021). The water from Rober Müser and Friedllicher Nachbar is respectively pumped at -445 m and -190 m from the surface.

Parameters	Robert Müser	Friedllicher Nachbar	Units
pH	6.95	9.82	
Eh - SHE	-143	8	mV
Conductivity	6.65	2.6	mS/cm
DOC	1.4	0.86	mg/L
TOC	1.4	0.88	mg/L
Na	1200	430	mg/L
K	24	20	mg/L
Ca	140	86	mg/L
Mg	55	44	mg/L
Ba	6.7	1.3	mg/L
Sr	2.3	0.1	mg/L
Fe	<0.02	3.25	mg/L
Mn ²⁺	0.25	3.61	mg/L
NH ₄ ⁺	1.78	0.71	mg/L
Cl	1700	300	mg/L

HCO ₃ ⁻	952	851	mg/L
SO ₄ ²⁻	75	221	mg/L
NO ₃ ⁻	<0.5	<0.2	mg/L
NO ₂ ⁻	<0.1	0.02	mg/L
P	0.14	<0.03	mg/L
Br	3.2	0.52	mg/L
F	0.44	0.25	mg/L
Si	7.53	7.47	mg/L
Li	0.6	0.28	mg/L
CO ₂ diss	94.6	129.8	mg/l
H ₂ S diss	2.33	> 0.1 (smell)	mg/l
S ₂ ⁻	4.75	0.15	mg/l
O ₂ diss	0.02	0.46	mg/l

Groundwaters from mines are rich in sodium, chloride, bicarbonates and sulfate. The salinity strongly evolves between both mine reservoirs and for this reason it is difficult to do extrapolation of the pilot water composition. Mine thermal energy storage process should have a low environmental impact on the mine reservoirs as they are already perturbed by human activities. The main issues concern the risk of pollution of upper aquifers. For this reason, water into the mines are pumped to maintain its level below the upper aquifers. The underground thermal energy storage process will not modify the water pumping and the wells have casings. Thus, the risk of contamination can be discarded. However, the water composition has to be monitored in shallow aquifer to detect any potential of leaks (in the well for example).

Despite the low impact of the mine thermal energy storage process on the environment, these underground systems can impact the process and its efficiency. Indeed, quick thermodynamic calculations with the Phreeqc software underline the risk of calcite and barite precipitations at 25°C. These precipitations could induce the scaling of the pipes and their plugging. These calculations should be refined with the real water composition of the pilot and also by considering the targeted temperatures of the cooled and heated reservoirs. Another issue concerns microbiology. Both mine waters contain a relatively high concentration of carbon (as bicarbonate or organic matter) and other chemical compounds (mainly sulfate) that could be metabolised by microorganisms. Production of corrosive gas like H₂S is thus possible. Analyses of the microbial diversity and their characterizations could be suitable to understand their potential effect on the process and the identification of potential mitigation solutions.

3.3.1 Conclusions and recommendations

Due to former mining activities, underground environment is already monitored to prevent any pollution. Continuous water pumping are performed to maintain the mine water level below the upper aquifers. Shallow aquifers have also to be monitored to prevent the risk of leaks. The mine thermal energy storage process should not impact more the environment than old mine activities. However, the water chemistry and the natural microorganisms could have strong effects on the process by promoting scaling or corrosion. Specific studies should be performed when targeted mines water will be characterised.

3.4 Plymouth

Early in the development of the Plymouth heat network project it was established that reinjection of water back into the aquifer was likely to be unsafe. This is because the aquifer is karst, with very unpredictable hydraulic behaviour and a shallow water table (5m to 10m below ground level beneath most of the area), such that the risk of subsurface flooding via natural and manmade pathways was judged to be significant. There are numerous lined and unlined wells deriving from the Elizabethan and Victoria eras via which groundwater under elevated heads due to reinjection could enter buildings, causing damage and risk to life e.g. Figure 21.

Having established that consumptive groundwater abstraction with a surface discharge back to the sea was the only viable groundwater configuration for the project, it was necessary to demonstrate that this was acceptable on environmental grounds. Historic accounts from the Elizabethan and Victorian eras confirmed that most historic wells became saline soon after installation and provided a firm indication that the fresh water resource within the coastal aquifer was very small. Furthermore, academic studies deriving from the 20th century established that many of these disused wells had strong tidal signals, indicating hydraulic connection with the sea. This legacy of saltwater occurrence in numerous wells from the 1500's provided a firm indication that the aquifers underlying the city of Plymouth had little or no value as a potable water source.



Figure 21. A Hand Dug Well Deriving from the Elizabethan Era – now an ornamental feature in a restaurant.

It was necessary to test the hypothesis that the aquifer underlying the project area had little or no value as a potable source with the environmental regulator. The premise for this was that the test well should produce saltwater very soon after commencement of testing and should attain and sustain a seawater composition thereafter. This was subsequently demonstrated where TDS concentrations in the pumped groundwater reached 30,000mg/l to 40,000mg/l within a few hours of the test start.

The pilot of Plymouth is located close to the coastline. As explained previously, the approach would be to pump water at 112 m of depth from the well called "PDLBHD(2)" and directly reject it into the sea (Figure 7). The water pumping into the aquifer will modify the hydrogeology of the system and thus the salt wedge (transition zone

between salt water (coming from the sea) and freshwater). A pumping test was already performed in the PDLBHD(2) well and highlighted an increase in the water salinity (Table 5).

Table 5: Evolution of the water composition of the PDLBHD(2) well during pumping test (Broadfoot, 2022).

Element	Unit	Sampling Date				
		21/06/2022 15:00	04/07/2022 14:12	05/07/2022 14:00	06/07/2022 15:37	06/07/2022 16:21
Calcium	mg/l	8	253	268	356	342
Magnesium	mg/l	2	693	992	916	867
Potassium	mg/l	<1	332	490	460	425
Sodium	mg/l	5	5530	8110	7860	7240
Total Hardness as CaCO ₃	mg/l	27.4	3790	5390	4950	4680
Total Sulphur as SO ₄	mg/l	<3	1590	2330	2030	1910
Chloride	mg/l	6	9760	10600	15100	13800

The intrusion of salt water inside the aquifer could impact other activities like agriculture or drinking water that need freshwater. However, several wells nearby the pilot could be used to monitor the evolution of the water composition (Figure 7) and should avoid contaminations and groundwater in this area is not used for such purposes. The increase in salinity could also have consequences on the infrastructure. An increase in the chloride concentration is known to increase corrosion processes. Another consequence of the intrusion of salt water will be a strong modification of the natural microbial communities. Further investigations will be necessary to determine if this microbial evolution could have an impact on the process (e.g. corrosion, plugging of the porosity...).

Rejection of water in the sea will probably also have consequences in the biogeochemistry of the seawater nearby the pipe, by modifying the temperature, the salinity and thus the (micro)organisms. This point has to be developed in other studies.

3.4.1 Conclusions and recommendations

The process will have a direct effect on the underground environment by modifying the water composition. However, this modification was planned and several boreholes were drilled to monitor the water composition and follow the perturbation. Analyses of the water composition and the microbial diversity would allow defining a natural baseline to better quantify the process effect.

The pumping test performed in 2022 should allow quantifying the process impact and adapt the monitoring network according to several scenarios of cooling and heating by hydrogeological modelling. This modelling would also allow defining studies to characterize the process impact on the (micro)organisms in sea and groundwater and conclude about potential consequences for the infrastructure (as corrosion).

3.5 Glasgow

This part of the environmental assessment focuses on the thermal storage of the pilots. Therefore, Glasgow pilot is not included in this section given that even though it uses waste water as an energy source, it does not have any underground thermal storage at the moment.

4 CO₂ emissions and renewable energy

4.1 System boundaries

The system boundaries used for calculating the CO₂ emissions and renewable energies of the pilot systems are defined in Figure 22. Dashed lines are not further treated and quantified for this environmental impact assessment. Any back-up systems that might be available are also not included in the assessment. Regarding electricity (from national grid and solar PV) net annual flows are indicated.

The system boundaries are inspired by the system boundaries of DHC systems as applied by Ivančić et al. (2021) and WEDISTRIC (2020). Adjustments are made based on the demarcation of this environmental impact assessment and the technologies currently used by the D2Grids pilot projects. The total energy demand is defined by the energy used by the buildings in kWh per year, to foresee in their heating-, cooling- and domestic hot water (DHW) demand. This energy is supplied by exchange of heat and cold between buildings and different technologies implemented within the D2Grids pilot projects (e.g. geothermal energy, streams of (waste) heat and renewable electricity sources). These sources of energy supply are included within the system boundaries.

Further, energy is supplied to the system from external energy sources (e.g. natural gas and electricity from the grid). The energy flows within the system, and from the outside to the system are quantified in kWh per year. Regarding CHP, it is considered within the system boundaries when it is delivering its entire production (electricity and heat) to the system. District heating systems connected to the 5GDHC pilot sites, which are not regarded as 5GDHC, and back-up systems (which could also include a CHP) will not be taken into account in this assessment. Regarding heat extraction from sewage (case of Glasgow pilot site), the sewage plant itself is falling outside the system boundaries and is considered as external source of heat.

In the schematic representation in Figure 22, the different heat pumps, chillers and substations present in the 5GDHC pilot systems are not shown separately, but represented as one 'energy center'. Energy flows showed with dashed lines and arrows in Figure 22 are not further treated and quantified for this environmental impact assessment. The exchange of heat and cold between buildings is roughly indicated, when possible. The term energy use in this assessment is defined as the amount of all energy that is not originating from exchange of heat and cold between buildings.

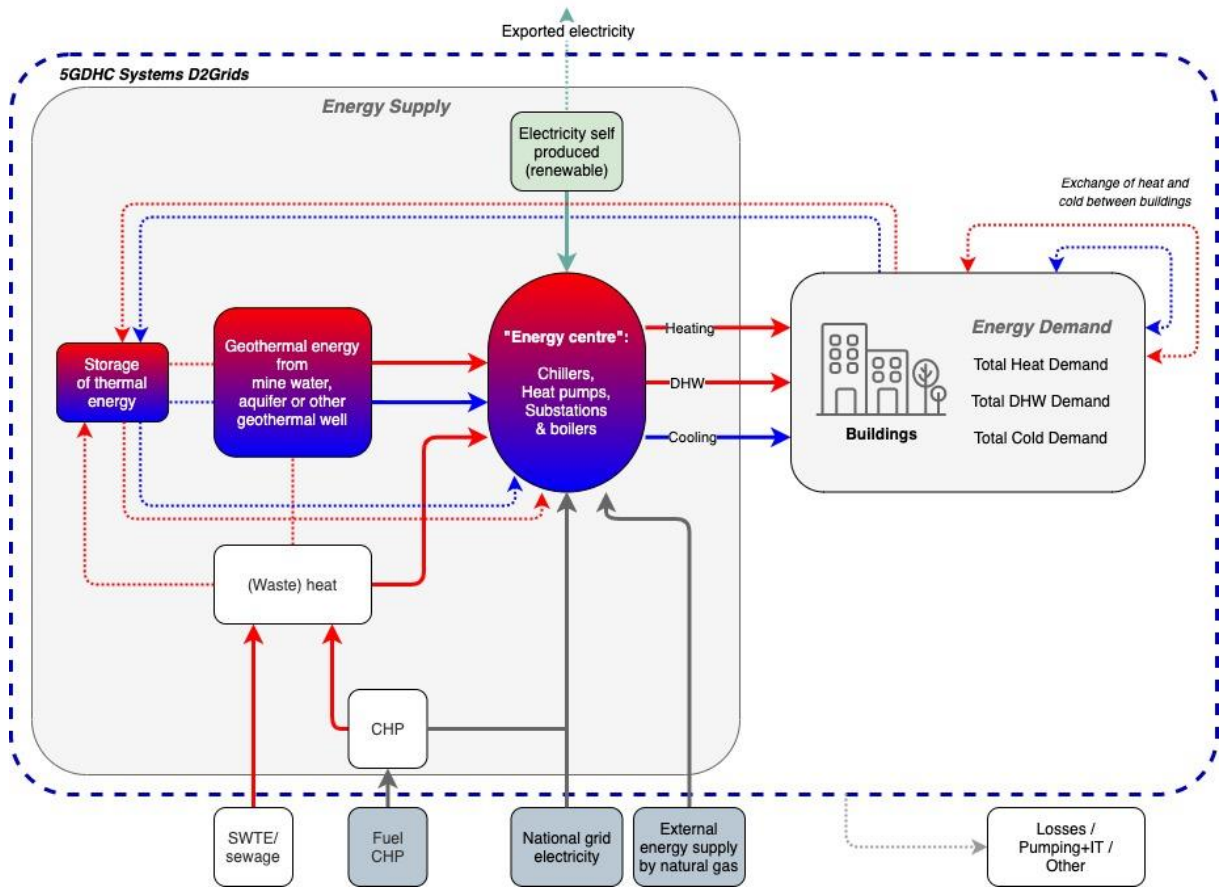


Figure 22. System boundaries of the 5GDHC pilot systems of D2Grids for assessing the environmental impacts of energy use.

4.2 CO₂ emissions of pilot sites

Using a CO_{2eq} emission factor of each source of energy, the yearly CO₂ equivalent (CO_{2eq}) emissions are calculated for the five different 5GDHC pilot projects (equation 1).

$$GHG_{total} = \sum(E_i * EF_i) \tag{Eq. 1}$$

Where:

GHG_{total} Total yearly CO_{2eq} emissions (tCO_{2eq}/year)
 E_i Energy supplied by each source of energy i per year (kWh/year)
 EF_i Emission factor CO_{2eq} of each source of energy i (tCO_{2e}/kWh)

Fossil emissions and biogenic emissions are considered separately. Fossil emissions are generated by the burning of fossil fuels or can be attributed to the burning of biomass, but are not part of the biogenic carbon cycle. Biogenic emissions are generated by the combustion of biomass (e.g. in a biomass boiler or by waste incineration). Regarding biogenic emissions, it is considered that all carbon sequestered in biomass during the growth is emitted in the form of biogenic CO₂ when combusted. These emissions are part of the biogenic carbon cycle and could be sequestered again by growing biomass.

Although considered as **non-renewable**, waste heat sources from a non-renewable primary energy source are in the calculation of CO_{2eq} emissions seen as a form of **reuse** of energy that would otherwise be wasted, they replace conventional energy sources and do not cause additional GHG emissions. In the calculation of the CO_{2eq} emissions, therefore, no emissions have been counted for waste heat sources.

In determining the CO_{2eq} emissions related to electricity use, the different national electricity production mixes for each pilot's country are used. For the calculation of the yearly CO_{2eq} emissions, only the direct GHG emissions from energy sources necessary for operation of the system are taken into account (emissions from upstream activities are not taken into account). The CO_{2eq} emission factor of each source of energy *i* (EF_i) is taken from the **D2Grids CO₂ calculation model** (available at 5gdhc.eu/development-toolkit).

Besides the yearly CO_{2eq} emissions, also the carbon intensity is calculated for the five pilot sites. The carbon intensity is the **ratio** between the total CO_{2eq} emissions of the 5GDHC system and the total energy demand for heating, cooling and domestic hot water (DHW) of the system. Heating, cooling and DHW may be produced differently and therefore have a different carbon intensity. In this research, differences in the production are not be taken into account, as heating, cooling and DHW are all necessary for the total system. Only the carbon intensity for the total system is calculated (equation 2).

$$C.I. = \frac{GHG_{total}}{E_{D_total}} \quad \text{Eq. 2}$$

Where:

C. I. Carbon intensity (tCO_{2eq}/kWh)
GHG_{total} Total yearly CO_{2eq} emissions (tCO_{2eq}/year)
E_{D_total} Total yearly energy demand for heating, cooling and DHW (kWh/year)

In this report, we do not include the impacts of local pollutants (SO_x, NO_x, PM_{2.5} and CO), as we focus on the impact of CO_{2eq} emissions. Moreover, when looking at local impacts pollutants, 5GDHC systems show favorable results compared to other heating and cooling systems. Nonetheless, the impacts of local pollutants were calculated for the pilots and can be found in the thesis document (Suijen, 2023).

Table 6 shows the total annual CO_{2eq} emissions and carbon intensity per pilot site. These emissions are based on emission factors for the national electricity production mixes in the five different countries.

Table 6 – Total annual CO_{2eq} emissions and carbon intensity per pilot

	<i>Total annual CO_{2eq} emissions (tCO_{2eq}/yr)</i>		<i>Carbon intensity (gCO_{2eq}/kWh)</i>	
	<i>With solar PV implemented</i>	<i>Without solar PV implemented</i>	<i>With solar PV implemented</i>	<i>Without solar PV implemented</i>
5GDHC pilot system				
Bochum	2706	2840	102	107
Brunssum	203	203	169	169
Paris-Saclay	2161	2163	79	79
Glasgow	-56*	49	-80*	69
Plymouth	348	362	68	71

* When solar PV implemented, for the pilot in Glasgow negative CO_{2eq} emissions are found, due to a net delivering of electricity to the national grid.

There is a separate column for emissions when solar panels are implemented in the pilots. As part of a second funding scheme, some of the D2Grids pilots will improve their network by installing solar panels inside their

system, this addition belongs to **WP.T4**. Those pilots are: Glasgow, Plymouth, and Paris-Saclay. Since the solar panels are not yet installed and connected to the system at the writing time of this assessment, design data was used. Additionally, the solar capacity from Bochum has been included in this assessment, but it is important to note that the financing for solar in Bochum will not come from D2Grids funding, therefore it is not part of **WP.T4**.

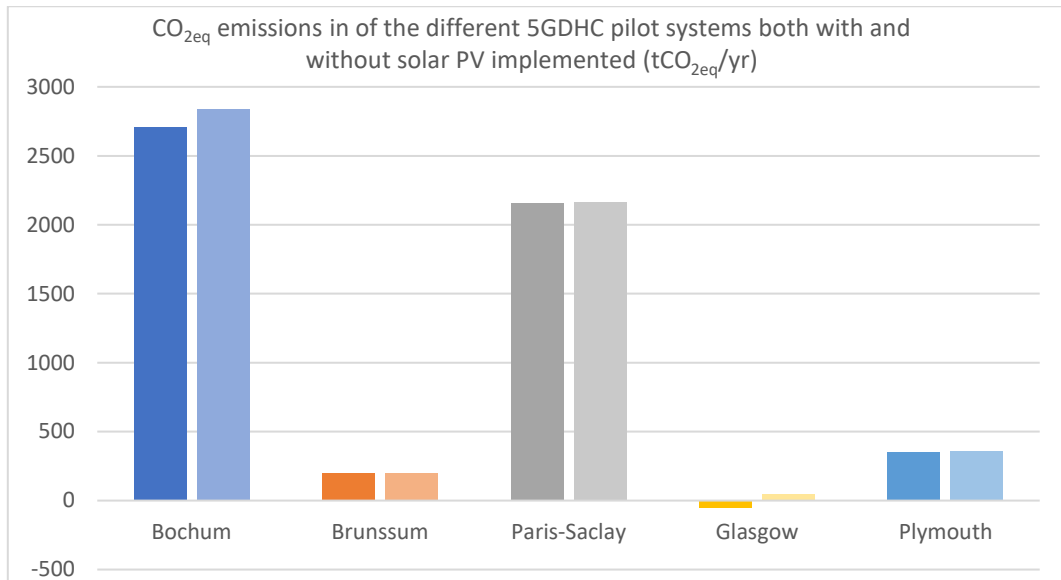


Figure 23. CO_{2eq} emissions in of the different 5GDHC pilot systems both with solar PV implemented (dark-shaded) and without (light-shaded) (tCO_{2eq}/yr)

The carbon intensities are regarding electricity calculated with emission factors for the different national electricity production mixes. The difference between CO_{2eq} emissions in the pilot is large due to the different sizes of each network. In order to compare the performance of the pilots against each other, in terms of emissions, we used the carbon intensity (tCO_{2eq}/kWh) as seen in Figure 24.

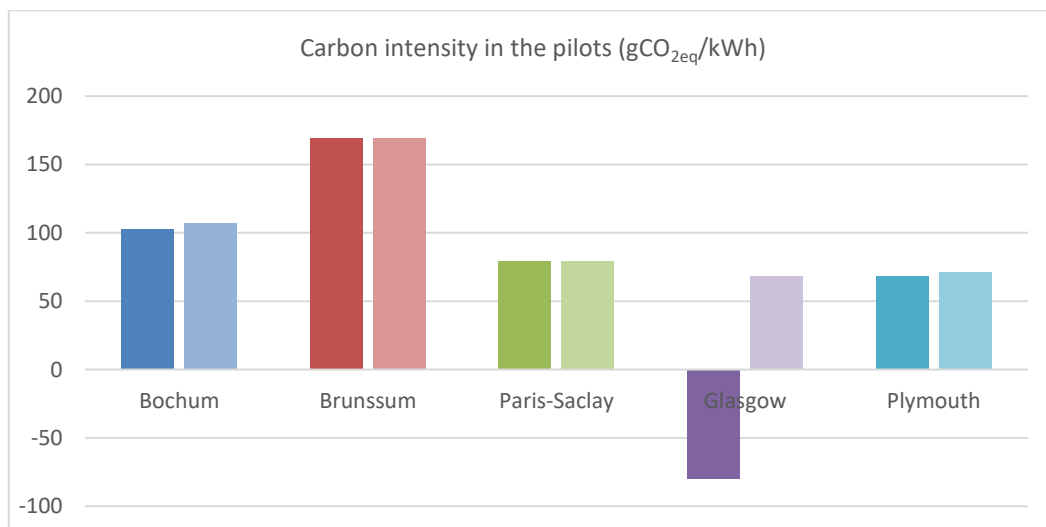


Figure 24. Carbon intensity of each pilot site (gCO_{2eq}/kWh). With solar PV implemented (dark-shaded) and without (light-shaded)

Light shaded are the ‘additional’ emissions (in gCO₂eq/kWh) when no solar PV would have been implemented, except for Glasgow, where the light shaded column gives the ‘actual’ carbon intensity when no solar PV would have been implemented (not additional).

4.2.1 CO₂ emissions avoidance

To calculate the emissions avoidance of the pilots by their use of a 5GDHC system, a comparison was made against a reference scenario based on a conventional district heating system. This system takes the following assumptions.

- Total cold demand is fulfilled with individual air conditioners powered by electricity.
- The total heat and DHW demand are fulfilled with individual natural gas boilers.
- In this scenario no heat and/or cold are exchanged between the buildings
- In determining the total energy demand in this scenario, the same energy demand as in the 5GDHC system (D2Grids pilot data) was taken.
- Total natural gas input for delivering heat and DHW is calculated using an assumed efficiency of the natural gas boilers of 90% (source assumption: Guillén-Lambea et al. (2021))
- The cooling COP for air conditioners is: 3,5
- No renewable electricity and heat sources are installed.

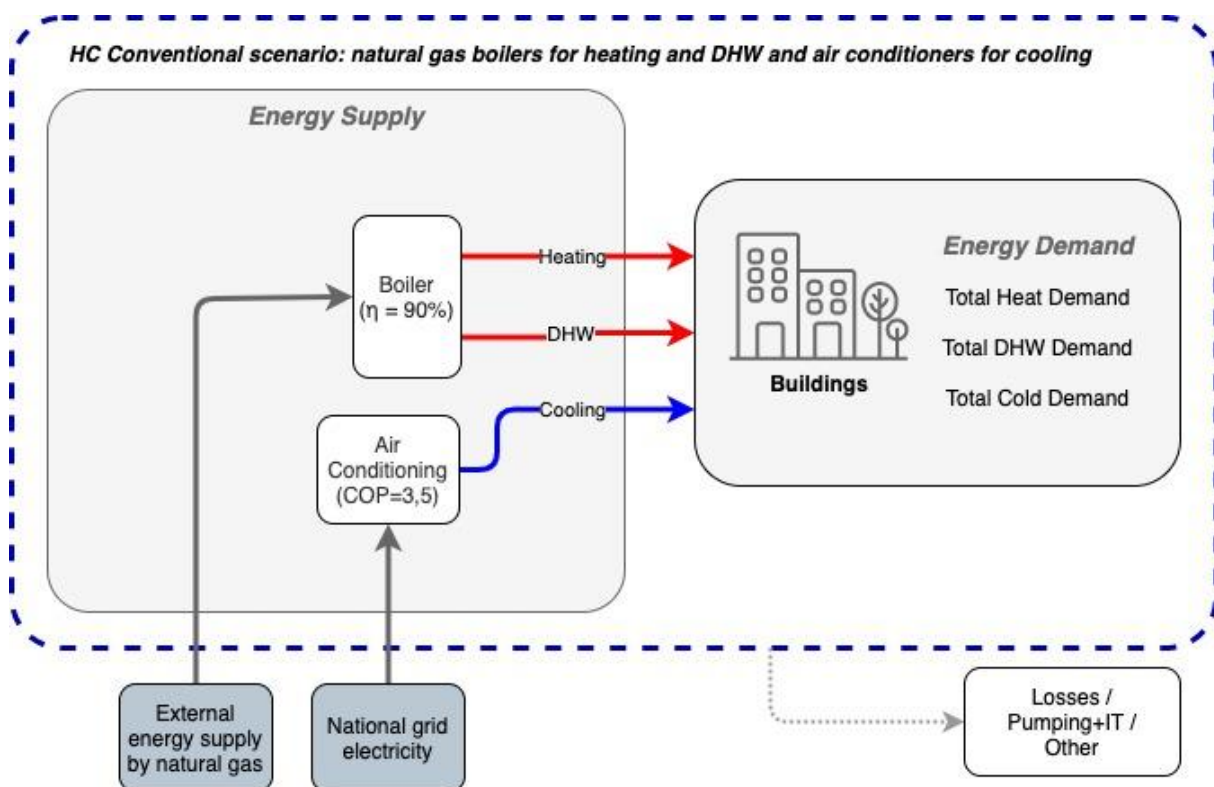


Figure 25. Schematic representation of a reference scenario with heating by individual natural gas boilers and cooling by individual air chillers.

The calculations were done with the tool developed in D2Grids (5gdhc.eu/development-toolkit) and resulted in the following figures:

Table 7. CO_{2eq} emissions reduced by implementing a 5GDHC system instead of a conventional system

	<i>Reduced annual CO_{2eq} emissions (tCO_{2eq}/yr) by implementing 5G</i>	<i>Additional annual CO_{2eq} emission reductions by implementing solar PV (tCO_{2eq}/yr).</i>
<i>Pilot</i>	Emission factor electricity from national grid	Emission factor electricity from national grid
Bochum	1.924	134
Brunssum	62	0
Paris-Saclay	3.180	3
Glasgow	95	105
Plymouth	582	14

CO_{2eq} emissions are reduced by implementing a 5GDHC system instead of a conventional system with individual gas boilers for heating and DHW and air conditioners for cooling. Regarding electricity, the emissions are presented both based on emission factors of the different national electricity production mixes. Further, emissions reductions due to the implementation of solar PV are shown separately.

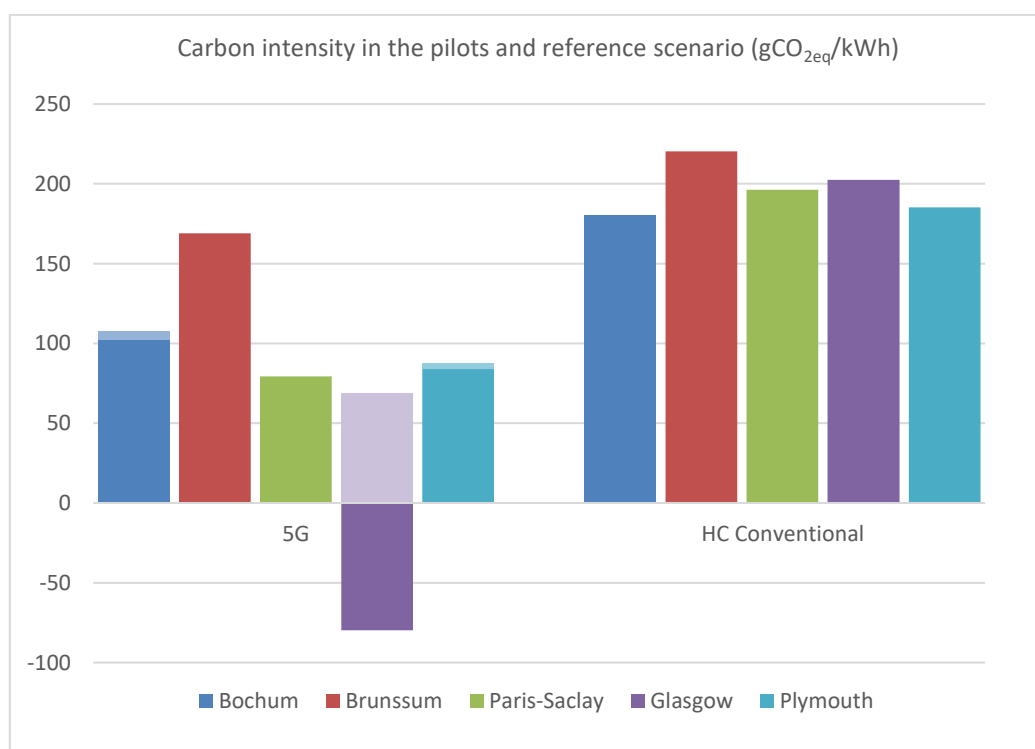


Figure 26. Carbon intensity (in gCO_{2eq} fossil/kWh) in the different scenarios for the 5GDHC pilot systems.

Comparison of emissions and other impact pollutants from the pilot sites against other reference scenarios can be found in the master's thesis (Suilen, 2023). The emissions avoidance from the pilots that are only attached to the D2Grids investments are calculated separately in another project deliverable.

4.3 Share of renewable energy

Renewable energy is defined as energy derived from non-fossil natural resources, that are constantly being replenished on a human timescale. Fossil fuels, like coal, oil and gas are considered as non-renewable sources, since these take hundreds of millions of years to form (European Commission, 2022).

In line with EU's Renewable Energy Directive (EU, 2018), within this research, the following energy sources are considered as renewable:

- Solar energy
- Wind energy
- Geothermal energy
- Aquathermia (thermal energy from surface/waste water)
- Hydropower
- Tidal energy
- Ambient energy
- Energy from biomass

For each energy source used by the different pilot projects, the share in the total energy use is calculated per pilot. Furthermore, the renewable energy ratio (*RER*) or share of renewable energy is calculated. This is done for thermal energy sources and electricity sources separately. All electricity coming from the grid will be considered as non-renewable, so only the RES installed in the project are taken into account. Waste heat sources from a non-renewable primary energy source, will be calculated separately. The share of renewable energy (thermal/electric) is also calculated.

As indicated in the methodology document developed in D2Grids deliverable (Del.LT.4.1), the calculation of renewable energy share in the pilots is done with the following formulas:

$$RER_{therm} = \frac{\sum RES_{therm,i}}{\sum E_{therm,i}} \quad \text{Eq. 3}$$

$$RER_{therm+R} = \frac{\sum RES_{therm,i} + \sum R_i}{\sum E_{therm,i}} \quad \text{Eq. 4}$$

$$RER_{elec} = \frac{\sum RES_{elec,i}}{\sum E_{elec,i}} \quad \text{Eq. 5}$$

$$RER_{Overall} = \frac{\sum RES_{elec,i} + \sum RES_{therm,i}}{\sum E_{elec,i} + \sum E_{therm,i}} \quad \text{Eq. 6}$$

Where:

RER_{therm}	Renewable energy ratio thermal energy sources (excl. $\sum R_i$)
$RER_{therm+R}$	Renewable and waste energy ratio thermal energy sources (incl. $\sum R_i$)
$RES_{therm,i}$	Energy supplied by each renewable thermal energy source i (excl. $\sum R_i$ per year (kWh/year)
R_i	Energy supplied by each waste heat source i from a non-renewable primary energy source per year (kWh/year)
$E_{therm,i}$	Total thermal energy supplied by each source of thermal energy i ($RES_{therm,i} + R_i +$ thermal energy from non-renewable sources) per year (kWh/year)
RER_{elec}	Renewable energy ratio electricity sources
$RES_{elec,i}$	Energy supplied by each renewable electricity source i per year (kWh/year)

$E_{elec,i}$ Total electric energy supplied by each source of electricity i (renewable plus non-renewable sources) per year (kWh/year)

 $RER_{overall}$ Renewable energy ratio including both thermal energy and electricity sources

Table 8 gives an overview of the different energy sources used by the 5GDHC pilot systems of D2GRIDS. In the 5HGDC pilot projects of D2Grids waste heat from a non-renewable primary energy sources (R) is not implemented. Regarding the renewable energy ratio (RER) or share of renewable energy of thermal energy, this means that in case of the assessed pilots the value of RER_{therm} and $RER_{therm+R}$ gives the same result.

Table 8. Overview energy sources used by the different D2Grids pilot projects (non-renewable sources, grey; renewable sources, green). Any backup systems used are not included in this table.

		Bochum	Brunssum	Paris-Saclay	Glasgow	Plymouth
Thermal energy	Natural gas (boilers/CHP)	x		x		
	Heat CHP (natural gas)	x				
	Geothermal well	x	x	x		x
	Waste heat from sewage				x	
Electricity	National grid	x	x	x	x	x
	Electricity from CHP	x				
	Solar PV	x		x	x	x

The renewable energy ratio (RER) or share of renewable energy per pilot is shown in Figure 27 for the thermal energy sources (in case of the pilot systems $RER_{therm} = RER_{therm+R}$). Here, we include the solar capacity that has been added to the Plymouth, Paris-Saclay, and Glasgow pilot systems as part of **WP.T4**.

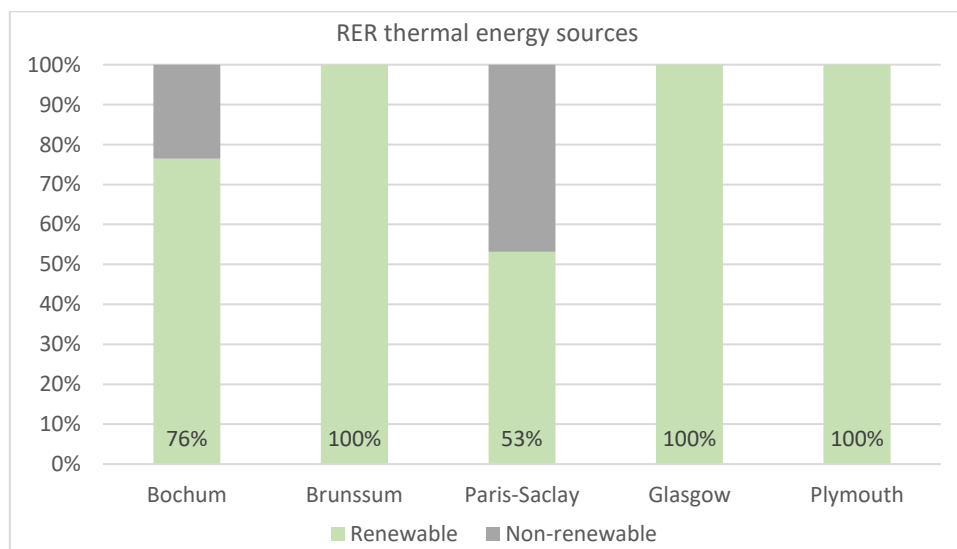


Figure 27. Share renewable thermal energy sources in the 5G scenario of the pilot systems

The share of renewable electricity sources (RER_{elec}) is shown in Figure 28. The share of renewable energy is depicted for the 5G scenario of the pilot systems. In the pilot of Glasgow a RER of over 100% is due to a greater amount of solar PV installed than their total electricity use. A more detailed calculation process and results can be found in the master's thesis (Suilen, 2023).

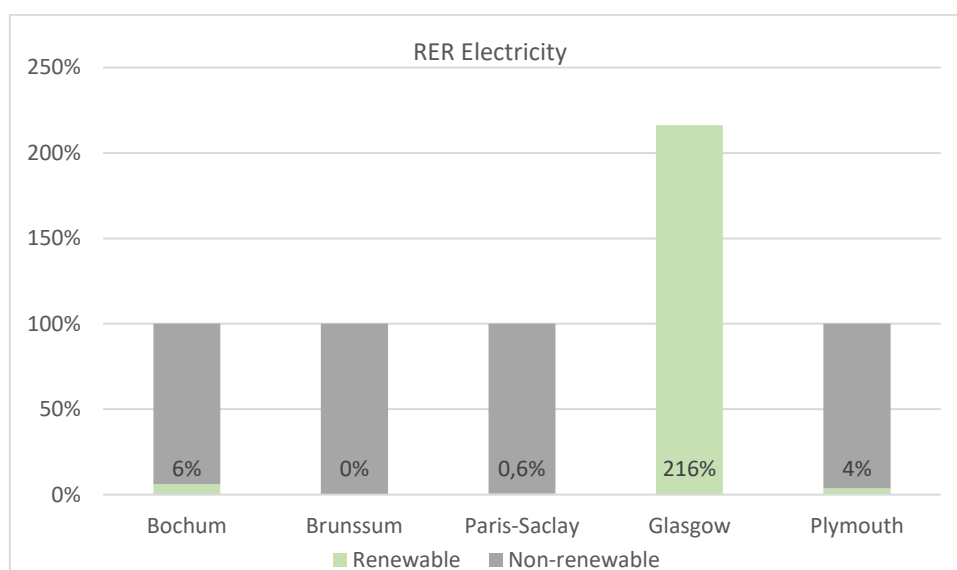


Figure 28. Share renewable electricity sources (RER_{elec}) in the 5G scenario of the pilot systems.

It is important to mention, that although grid electricity is not considered as renewable in this study, for the pilot in Bochum, all the electricity fed into the system from the power grid (external), used to meet the electricity requirements of the geothermal heating and cooling supply (pumps, etc.) will be 100% green electricity through green certificates.

4.4 Conclusions and recommendations

Besides lowering CO_{2eq} emissions compared to conventional heating and cooling techniques, 5GDHC systems also contribute to reducing dependency on fossil fuels and using local energy sources. Regarding thermal energy sources, the pilot sites of Brunssum, Glasgow and Plymouth operate ‘natural gas-free’ and 100% on renewable thermal energy sources, using local geothermal energy and thermal energy recovery from waste water. The pilots of Bochum and Paris-Saclay operate for respectively 76% and 53% on renewable thermal energy sources. Including solar PV as well, with an overall share of renewable energy implemented of 54-132% four of the five pilot sites meet both current and future EU targets regarding renewable energy implementation. The pilot of Paris-Saclay, has at this moment an overall share of renewable energy implemented of 35%. Current EU targets are met, targets that are likely to apply in future are expected to be met in 2023, when the use of geothermal energy can be further expanded in the pilot in Paris-Saclay.

Table 9 – Performance of the 5GDHC pilot systems regarding different indicators.

	<i>Bochum</i>	<i>Brunssum</i>	<i>Paris-Saclay</i>	<i>Glasgow</i>	<i>Plymouth</i>
Carbon intensity (in $kgCO_{2eq}/kWh$)*	107	169	79	69	71
Overall share of RES implemented (in %)	54%	58%	35%	132%	69%
Total yearly cooling demand as percentage of the total energy demand	39%	6%	15%	15%	26%
Total yearly heating demand as percentage of the total energy demand	61%	94%	85%	85%	74%
District DOC**	0,64	0,07	0,17	0,18	0,35
Ratio total electricity use / total energy demand	0,22	0,45	0,35	0,31	0,32

* Regarding electricity, the calculations are based on national emission factors and no solar PV implemented.

** Ratio of the total yearly cooling demand and the total yearly heating demand (incl. DHW). Measures overlap between heating and cooling demand.

The performance of the different 5GDHC pilot projects is dependent on several factors (technical configuration of the system, network configuration, demand profile, location and climate). Therefore, comparison of the different pilot projects is not possible without considering this dependency. However, based on the indicators and results shown in Table 9, the pilots of Bochum and Plymouth show the most favorable when considering potential exchange of energy flows, as they have the best match of heating and cooling demands (District DOC). Regarding carbon intensity and RES implemented, Glasgow and Plymouth are having the most favorable results. Brunssum has a relatively low cooling demand, with a DOC of 0,07. With respect to the ratio of total electricity use and total energy demand a relatively low value is found in Bochum and a relatively high value in Brunssum.

In order to specifically assess the environmental impacts of 5GDHC systems and have a comparison to the previous generation district heating systems, namely 4GDHC, the exchange of heat and cold between buildings plays an essential role. In future research, if information about the exchange of heat and cold becomes available, this should be used. Otherwise, detailed modelling could be a possible approach to obtain a better insight in the effects of exchange of heat and cold between buildings. Possibilities to incorporate in such a model would be the changing heating and cooling demand over time, the spatial distribution of the different heat and cold sources, the size of the network and possible scenarios with certain amounts of exchange of heat and cold between buildings on building level, including possible losses.

5 Impacts of heat pumps

The assessment of impacts from heat pumps shown in this section, as well as any information regarding heat pumps in this document, has been extracted from the master's thesis, Suilen (2023), where more information can also be found.

As environmental impacts of heat pumps, only possible emissions of HFCs are further considered in this research. The type and amount of heat pumps used or planned to be used in the pilot projects with 5GDHC are inventoried, by sending out a questionnaire to the different 5GDHC pilot projects. Also inventoried is whether the heat pumps use a refrigerant based on HFCs, if a refill of this refrigerant was necessary and if so, how much. The results of this inventory can be found in the thesis document, Suilen (2023).

With the limited information available, a rough estimation is done about the expected emissions of HFCs due to the use of heat pumps by the different pilots. None of the 5GDHC pilot systems could provide concrete information about whether leakage of HFCs actually takes place. For the pilot of Glasgow, no information is available about the heat pumps used or planned to be used at the time of writing this report. For the pilots of Bochum and Plymouth an indication is available of the heat pumps planned to be used. For these pilots it is not yet known whether the heat pumps in the pilots will contain a refrigerant based HFCs. In the calculation of expected HFC emissions, it is assumed that these heat pumps will indeed contain HFCs.

For the pilots of Bochum, Paris-Saclay and Plymouth the heat pumps used or planned to be used are divided over the different size categories (as defined by Eunomia (2014)) as shown in Table 10. For the pilot in Brunssum exact types of heat pumps are known, so refrigerant used and refrigerant charge could be retrieved. For the pilot in Brunssum an estimation of HFC emissions is derived, directly from this information. The total estimated emissions of HFCs in CO_{2eq} emissions per pilot, based on an assumed annual refrigerant leakage rate of 3,8% (Eunomia, 2014), are shown in Table 11. The percentage of CO_{2eq} emissions due to leakage of HFCs from heat pumps of the total CO_{2eq} emissions of the 5GDHC system is also shown in this table and is roughly estimated to be 0,1 – 11% for the assessed pilots.

Table 10 shows the amount of heat pumps with a refrigerant based on HFCs, used or planned to be used by the different 5GDHC pilot systems, divided over the different size categories as defined by (Eunomia, 2014). It is not yet known if the heat pumps planned to be used in the future will contain refrigerants based on HFCs (Bochum and Plymouth), therefore it is assumed that these heat pumps will indeed contain HFCs.

Table 10 – Amount of heat pumps with a refrigerant based on HFCs

		<i>Amount of heat pumps with refrigerant based on HFCs</i>		
	<i>Size</i>	<i>Bochum</i>	<i>Paris-Saclay</i>	<i>Plymouth</i>
Non-domestic Heat pumps*	<i>Less than 50 kW</i>	0	0	0
	<i>50 - 250 kW</i>	1	0	4
	<i>250 kW or more</i>	3	24	1

Table 11 shows the estimated emissions of HFCs in CO_{2eq} emissions, and the percentage of CO_{2eq} emissions due to leakage of HFCs from heat pumps, based from the total CO_{2eq} emissions of the 5GDHC system per pilot with an assumed annual refrigerant leakage of 3,8%. For the pilots of Bochum, Paris-Saclay and Plymouth, assumed is usage of refrigerant R32 or R410a. For the pilot in Brunssum, the refrigerant and charge of the used heat pumps is searched and only total estimated CO_{2eq} emissions are given.

Table 11 – Total estimated emissions of HFCs in CO_{2eq} emissions and percentage of CO_{2eq} emissions due to leakage of HFCs

	<i>Total estimated HFC emissions in CO_{2eq} emissions due to leakage of refrigerant (tCO_{2eq}/yr)</i>	<i>HFC emissions in percentage of total CO_{2eq} emissions 5G system*</i>
Bochum	3 - 9	0,1 – 0,4 %
Brunssum	19	11 %
Paris-Saclay	18 - 56	0,4 – 1 %
Glasgow	No information available within the time of research.	
Plymouth	3 - 11	0,8 – 2 %

*Total CO_{2eq} emissions 5G system are calculated without implementation of solar PV and regarding electricity based on a European average emission factor.

Previously, we calculated the reduced CO_{2eq} (fossil) emissions given by implementing a 5GDHC system instead of a conventional system with individual gas boilers for heating and DHW and air conditioners for cooling (The calculations were done with the tool developed in D2Grids (5gdhc.eu/development-toolkit) and resulted in the following figures:

Table 7). The estimated HFC emissions as percentage of these emission reductions are presented in Table 12 and range from 0,2 - 17%. In the table, results show the estimated emissions of HFCs in percentage of CO_{2eq} emission reduction by implementing a 5GDHC system instead of a conventional heating and cooling scenario.

Table 12 – Estimated emissions of HFCs in percentage of CO_{2eq} emission reduction

<i>Pilot</i>	<i>HFC emissions in percentage of CO_{2eq} emission reduction* by implementing a 5G system instead of conventional heating and cooling</i>
Bochum	0,2 – 0,5 %
Brunssum	17 %
Paris-Saclay	1,4 – 4,3 %
Glasgow	No information available within the time of research.
Plymouth	0,7 – 2 %

**Emission reduction values are taken of a situation without implementation of solar PV and regarding electricity based on a European average emission factor.*

In general, between 2014 and 2020, HFC emissions in the European Union have declined, although countries outside the EU still show an increase in HFC emissions (United Nations, 2022). This coincides with the current EU regulation (2022) to control emissions from fluorinated greenhouse gases, including HFCs (F-gas Regulation), which applies from 2015. Updated regulation is currently under negotiation. Main points of this regulation are:

- Limiting the total amount of the most important fluorinated greenhouse gases that can be sold.
- Banning the use of fluorinated greenhouse gases in new types of equipment, where less harmful alternatives are available.
- Preventing emissions by maintenance checks and recovery of the gases at the equipment's end of the life. Hereby, equipment containing fluorinated greenhouse gases in quantities of 5 tons of CO_{2eq} or more, fall under the obligation of leakage checks and record keeping (Article 4 & 6).
Except for the booster heat pumps in Brunssum, this would apply for all heat pumps indicated to be used so far in the 5GDHC pilot projects.

5.1.1 Conclusions and recommendations

Since none of the 5GDHC pilots could provide data on real experiences with leakage of refrigerants, the determinations of possible HFC emissions are assumption based only. Also, since pilot sites are still under construction and a major part of the heat pumps that will be installed still have to be put out to tender, detailed information about the heat pumps is missing.

Since literature providing a concrete quantification of HFC leakage from heat pumps is sparse, assumptions about leakage rates are based on one report only, namely Eunomia (2014). Eunomia (2014) conclude in their report that CO_{2eq} levels of emissions from leakage are small relative to the total emissions reductions which might be delivered by using heat pump technologies. The results of this assessment seem to be in line with the findings of Eunomia (2014). However, the results are only estimation based and show a wide range of possible HFC emissions (0,2 - 17%).

Furthermore, since this quantification is not based on data from real experiences, but on assumptions only and only few systems are assessed, it is not possible to draw general conclusions. Repeating this assessment in the near future, when more experience has been gained in the pilot sites with possible leakage of HFCs and include a broader range heat pump users in a study, could provide more insight in the actual effect of the leakage of refrigerants through the use of heat pump technology. On the other hand, since heat pump technology will continue developing and (EU) regulations aim to limit the use of HFCs, it is expected that the impact of HFC emissions will further decrease in future. Nevertheless, it is recommended and also obligated by regulations, to reduce the environmental impact of heat pumps. This will be by, if possible, opting for heat pumps without HFCs and avoiding leakage of refrigerant through monitoring, early leak detection and quick repair.

6 References

- 5GDHC Masterplan & Technical Specifications - Paris-Saclay's pilot site (No. Deliverable D.T3.1.2 & D.T3.1.3), 2020. , D2-Grids project. EPA Paris-Saclay.
- Blanc, P., Lassin, A., Piantone, P., Azaroual, M., Jacquemet, N., Fabbri, A., Gaucher, E.C., 2012. Thermoddem: A geochemical database focused on low temperature water/rock interactions and waste materials. *Appl. Geochem.* 27, 2107–2116. <https://doi.org/10.1016/j.apgeochem.2012.06.002>
- Broadfoot, H., 2022. Bath Street Plymouth Pumping Test Factual Report (No. P3043-605– 001). WJ Uk.
- Buffa, S., Cozzini, M., D'Antoni, M., Baratieri, M., & Fedrizzi, R. (2019). 5th generation district heating and cooling systems: A review of existing cases in Europe. *Renewable and Sustainable Energy Reviews*, 104, 504–522. <https://doi.org/10.1016/j.rser.2018.12.059>
- Escudié, F., Auer, L., Bernard, M., Mariadassou, M., Cauquil, L., Vidal, K., Maman, S., Hernandez-Raquet, G., Combes, S., Pascal, G., 2018. FROGS: Find, Rapidly, OTUs with Galaxy Solution. *Bioinforma. Oxf. Engl.* 34, 1287–1294. <https://doi.org/10.1093/bioinformatics/btx791>
- Eunomia. (2014). Impacts of Leakage from Refrigerants in Heat Pumps. Eunomia Research & Consulting Ltd and the Centre for Air Conditioning and Refrigeration Research (London Southbank University).
- European Commission. (2022). *Renewable energy targets*. Renewable Energy Targets. https://energy.ec.europa.eu/topics/renewable-energy/renewable-energy-directive-targets-and-rules/renewable-energy-targets_en
- European Union. (2018). Directive (EU) 2018/844 of the European Parliament and of the Council of 30 May 2018 amending Directive 2010/31/EU on the energy performance of buildings and Directive 2012/27/EU on energy efficiency (Text with EEA relevance).
- Fardeau, M.-L., Barsotti, V., Cayol, J.-L., Guasco, S., Michotey, V., Joseph, M., Bonin, P., Ollivier, B., 2010. *Caldinitratiruptor Microaerophilus*, gen. nov., sp. nov. Isolated from a French Hot Spring (Chaudes-Aigues, Massif Central): a Novel Cultivated Facultative Microaerophilic Anaerobic Thermophile Pertaining to the Symbiobacterium Branch within the Firmicutes. *Extremophiles* 14, 241–247. <https://doi.org/10.1007/s00792-010-0302-y>
- Fremont, F., 2021. Doublet géothermique de la ZAC du Moulon - Réhabilitation du doublet de puits GMOU1 et GMOU2 - Rapport de fin d'opérations. (No. DCE21009). Geofluid.
- Galushko, A., Kuever, J., 2020. *Desulfobulbaceae*, in: Trujillo, M.E., Dedysh, S., DeVos, P., Hedlund, B., Kämpfer, P., Rainey, F.A., Whitman, W.B. (Eds.), *Bergey's Manual of Systematics of Archaea and Bacteria*. Wiley, pp. 1–4. <https://doi.org/10.1002/9781118960608.fbm00194.pub2>
- Garrity, G.M., Bell, J.A., Lilburn, T., 2015. *Pseudomonadales*, in: *Bergey's Manual of Systematics of Archaea and Bacteria*. Wiley, pp. 1–1. <https://doi.org/10.1002/9781118960608.obm00102>
- Gaur, A. S., Fitiwi, D. Z., & Curtis, J. (2021). Heat pumps and our low-carbon future: A comprehensive review. *Energy Research & Social Science*, 71, 101764. <https://doi.org/10.1016/j.erss.2020.101764>
- Guillén-Lambea, S., Carvalho, M., Delgado, M., & Lazaro, A. (2021). Sustainable enhancement of district heating and cooling configurations by combining thermal energy storage and life cycle assessment. *Clean Technologies and Environmental Policy*, 23(3), 857–867. <https://doi.org/10.1007/s10098-020-01941-9>
- Häusler, S., Weber, M., Siebert, C., Holtappels, M., Noriega-Ortega, B.E., De Beer, D., Ionescu, D., 2014. Sulfate Reduction and Sulfide Oxidation in Extremely Steep Salinity Gradients Formed by Freshwater Springs Emerging into the Dead Sea. *FEMS Microbiol. Ecol.* 90, 956–969. <https://doi.org/10.1111/1574-6941.12449>
- Ivančić, A., Romanić, J., Salom, J., & Cambroner, M.-V. (2021). Performance Assessment of District Energy Systems with Common Elements for Heating and Cooling. *Energies*, 14(8), 2334. <https://doi.org/10.3390/en14082334>
- Iino, T., 2018. *Ignavibacteriales*, in: *Bergey's Manual of Systematics of Archaea and Bacteria*. Wiley, pp. 1–2. <https://doi.org/10.1002/9781118960608.obm00141>
- Kalyuzhnaya, M.G., De Marco, P., Bowerman, S., Pacheco, C.C., Lara, J.C., Lidstrom, M.E., Chistoserdova, L., 2006. *Methyloversatilis Universalis* gen. nov., sp. nov., a Novel Taxon within the Betaproteobacteria Represented by Three Methylophilic Isolates. *Int. J. Syst. Evol. Microbiol.* 56, 2517–2522. <https://doi.org/10.1099/ijs.0.64422-0>

- Manz, W., Kalmbach, S., Szewzyk, U., 2015. *Incertae Sedis I. Aquabacterium*, in: Bergey's Manual of Systematics of Archaea and Bacteria. Wiley, pp. 1–6. <https://doi.org/10.1002/9781118960608.gbm00953>
- Marinelli, S., Lollo, F., Gamberini, R., & Rimini, B. (2019). Life Cycle Thinking (LCT) applied to residential heat pump systems: A critical review. *Energy and Buildings*, 185, 210–223. <https://doi.org/10.1016/j.enbuild.2018.12.035>
- Mégniën, C., Mégniën, F., 1980. Synthèse géologique du Bassin de Paris (No. Mémoire du BRGM n°101). BRGM.
- RAG, A., n.d. Heinrich, Friedlicher Nachbar, Robert Müser: Die Standorte der Grubenwasserhaltungen an der Ruhr.
- Raoult, Y., Boulègue, J., Lauerjat, J., Olive, P., 1997. Contribution de la géochimie à la compréhension de l'hydrodynamisme de l'aquifère de l'Albien dans le Bassin de Paris. *Comptes Rendus Académie Sci. - Ser. IIA - Earth Planet. Sci.* 325, 419–425. [https://doi.org/10.1016/S1251-8050\(97\)81159-7](https://doi.org/10.1016/S1251-8050(97)81159-7)
- Rast, P., Glöckner, I., Boedeker, C., Jeske, O., Wiegand, S., Reinhardt, R., Schumann, P., Rohde, M., Spring, S., Glöckner, F.O., Jogler, C., Jogler, M., 2017. Three Novel Species with Peptidoglycan Cell Walls form the New Genus *Lacunisphaera* gen. nov. in the Family Opitutaceae of the Verrucomicrobial Subdivision 4. *Front. Microbiol.* 8. <https://doi.org/10.3389/fmicb.2017.00202>
- Schüler, D., Schleifer, K., 2015. *Magnetospirillum*, in: Bergey's Manual of Systematics of Archaea and Bacteria. Wiley, pp. 1–7. <https://doi.org/10.1002/9781118960608.gbm00893>
- Seibt, A., 2021. Bestimmung der chemisch-physikalischen Eigenschaften von Grubenwasser (Interreg: D2Grids Project FUW Bochum). BWG Geochemische Beratung GmbH and Stadtwerke Bochum Holding GmbH.
- Suilen, J. (2023). Environmental impact assessment of 5th generation district heating and cooling systems (Master's thesis). Open Universiteit, The Netherlands. <https://ojs.ou.nl/ojs/index.php/eJES/article/view/194>
- Ungemach, P., Souque, C., 2021. Etude de la problématique de réinjection dans les formations sablo-argileuses de l'Albien du bassin parisien (No. DCE21144). Geofluid.
- United Nations. (2022). Hydrofluorocarbons (HFCs) Emissions, in kilotonne CO2 equivalent. <http://data.un.org/Data.aspx?d=GHG&f=seriesID%3AHFC>
- Vancanneyt, M., Segers, P., Abraham, W.-R., Vos, P., 2005. *Brevundimonas*, in: Bergey's Manual® of Systematic Bacteriology. Springer-Verlag, New York, pp. 308–316. https://doi.org/10.1007/0-387-29298-5_80
- Vuillaume, Y., 1971. Application des méthodes isotopiques et hydrochimiques à l'étude de la nappe de l'Albien du bassin de Paris (No. 71 SGN 304 HYD). BRGM.
- WEDISTRICT. (2020). *D2.2 KPI's definition*. <https://www.wedistrict.eu/resources/>
- Willems, A., Gillis, M., 2015. *Comamonadaceae*, in: Bergey's Manual of Systematics of Archaea and Bacteria. Wiley, pp. 1–6. <https://doi.org/10.1002/9781118960608.fbm00182>
- Wu, K., Cheng, L., 2021. *Ruminiclostridium*, in: Trujillo, M.E., Dedysh, S., DeVos, P., Hedlund, B., Kämpfer, P., Rainey, F.A., Whitman, W.B. (Eds.), Bergey's Manual of Systematics of Archaea and Bacteria. Wiley, pp. 1–11. <https://doi.org/10.1002/9781118960608.gbm01924>